© 2015. Published by The Company of Biologists Ltd | Development (2015) 142, 1228-1241 doi:10.1242/dev.111617

RESEARCH ARTICLE

STEM CELLS AND REGENERATION

p53 enables metabolic fitness and self-renewal of nephron progenitor cells

Yuwen Li[1,*], Jiao Liu[1,2,*], Wencheng Li[3], Aaron Brown[4], Melody Baddoo[5], Marilyn Li[6], Thomas Carroll[7], Leif Oxburgh[4], Yumei Feng[3] and Zubaida Saifudeen[1,2,‡]

ABSTRACT

Contrary to its classic role in restraining cell proliferation, we demonstrate here a divergent function of p53 in the maintenance of self-renewal of the nephron progenitor pool in the embryonic mouse kidney. Nephron endowment is regulated by progenitor availability and differentiation potential. Conditional deletion of *p53* in nephron progenitor cells (*Six2Cre*$^{+}$*;p53*$^{fl/fl}$) induces progressive depletion of Cited1^{+}/Six2^{+} self-renewing progenitors and loss of cap mesenchyme (CM) integrity. The Six2(p53-null) CM is disorganized, with interspersed stromal cells and an absence of a distinct CM-epithelia and CM-stroma interface. Impaired cell adhesion and epithelialization are indicated by decreased E-cadherin and NCAM expression and by ineffective differentiation in response to Wnt induction. The *Six2Cre*$^{+}$*;p53*$^{fl/fl}$ cap has 30% fewer Six2(GFP^{+}) cells. Apoptotic index is unchanged, whereas proliferation index is significantly reduced in accordance with cell cycle analysis showing disproportionately fewer *Six2Cre*$^{+}$*;p53*$^{fl/fl}$ cells in the S and G2/M phases compared with *Six2Cre*$^{+}$*;p53*$^{+/+}$ cells. Mutant kidneys are hypoplastic with fewer generations of nascent nephrons. A significant increase in mean arterial pressure is observed in early adulthood in both germline and conditional Six2(p53-null) mice, linking p53-mediated defects in kidney development to hypertension. RNA-Seq analyses of FACS-isolated wild-type and Six2(GFP^{+}) CM cells revealed that the top downregulated genes in *Six2Cre*$^{+}$*;p53*$^{fl/fl}$ CM belong to glucose metabolism and adhesion and/or migration pathways. Mutant cells exhibit a ~50% decrease in ATP levels and a 30% decrease in levels of reactive oxygen species, indicating energy metabolism dysfunction. In summary, our data indicate a novel role for p53 in enabling the metabolic fitness and self-renewal of nephron progenitors.

KEY WORDS: P53, Self-renewal, Nephron, Metabolism, Progenitors

INTRODUCTION

Congenital or acquired nephron deficit results in hypertension and chronic kidney disease (Brenner et al., 1988; Hoy et al., 2008), a major health problem worldwide. Nephron endowment at birth is determined, in part, by the availability of the nephron progenitor cells (NPCs) and their efficient differentiation into nephrons. Nephron abundance varies amongst individuals and populations, with a demonstrated influence of genetics and maternal nutritional status on nephron number in humans (Benz and Amann, 2010; Hoy et al., 2006; Luyckx and Brenner, 2010; Wlodek et al., 2008). Self-renewal of NPCs ensures a supply of cells for nephrogenesis until the cessation of nephrogenesis at postnatal day 4 in mice and at 35 weeks of gestation in humans (Hartman et al., 2007; Rumballe et al., 2011). The nephron progenitor niche includes the cap mesenchyme (CM), in which the NPCs reside, and provides extrinsic cues, such as nutrients and morphogens that drive cell intrinsic signaling and metabolic pathways, to promote the availability of NPCs for subsequent nephrogenesis. Renewal of the NPC pool is dependent upon ureteric bud (UB) secreted Wnt9b-β-catenin signaling to Six2^{+}/Cited1^{+} NPCs, as well as FGF, EGF and BMP signaling pathways, with their genetic inactivation resulting in defects in NPC renewal and differentiation (Brown et al., 2011, 2013; Karner et al., 2011).

Fate mapping studies with Cited1-CreER^{T2} and Six2-GFPCreERT (*Six2*^{GCE}) mice have demonstrated that the Cited1^{+}/Six2^{+} subcompartment marks the definitive self-renewing nephron progenitor domain that will differentiate to the inducible Cited1^{-}/Six2^{+} and Wnt4^{+}/β-catenin^{+}/Lef1^{+} cells to form nascent nephrons (Boyle et al., 2008; Kobayashi et al., 2008; Mugford et al., 2009). Expression of Six2 is essential to maintain the progenitor state (Self et al., 2006). Loss of self-renewal, proliferative or survival capacity in the Cited1^{+}/Six2^{+} CM will result in a diminished cap and a smaller NPC pool.

In its canonical role as a tumor suppressor, p53 (*Tp53* – Mouse Genome Informatics) plays a key role in cell fate regulation by transcriptionally regulating genes that control cell cycle arrest, DNA repair, apoptosis or senescence, thus limiting the propagation of cells with damaged genomes (Amariglio et al., 1997; Asker et al., 1999; Aylon and Oren, 2007; Vousden and Prives, 2009). p53 also regulates genes in metabolic pathways such as oxidative respiration and glycolysis for energy generation and glucose homeostasis, genes in cell adhesion and migration via Rho signaling pathways, genes regulating polarity of cell division, and autophagy (Armata et al., 2010; Balaburski et al., 2010; Buchakjian and Kornbluth, 2010; Cicalese et al., 2009; Gadea et al., 2007; Olovnikov et al., 2009; Tasdemir et al., 2008). Recent studies in hematopoietic, mammary and neuronal stem cells link p53 with the regulation of self-renewal potential (Cicalese et al., 2009; Liu et al., 2009; Meletis et al., 2006). Although data from some tissue lineages indicates that p53 restricts self-renewal capacity and the size of the stem and/or progenitor pool, data from mouse embryonic stem cells suggest that p53 serves as a positive regulator of self-renewal, by maintaining strict genome integrity quality-control that is essential in proliferative self-renewing progenitor populations

[1]Section of Pediatric Nephrology, Department of Pediatrics, Tulane University Health Sciences Center, New Orleans, LA 70112, USA. [2]The Hypertension and Renal Centers of Excellence, Tulane University Health Sciences Center, New Orleans, LA 70112, USA. [3]Department of Biomedical Science, Colorado State University, Fort Collins, CO 80523, USA. [4]Center for Molecular Medicine, Maine Medical Center Research Institute, Scarborough, ME 04074, USA. [5]Tulane Cancer Center. [6]Department of Molecular and Human Genetics, Baylor College of Medicine, Houston, TX 77030, USA. [7]Department of Internal Medicine (Nephrology) and Cell Biology, University of Texas Southwestern Medical Center, Dallas, TX 75390, USA.
*These authors contributed equally to this work

‡Author for correspondence (zubisaif@tulane.edu)

Received 16 April 2014; Accepted 12 February 2015

Development (2015) 142, 1228-1241 doi:10.1242/dev.111617

(Lee et al., 2010; Schoppy et al., 2010; Xu, 2005). Therefore, the requirement of p53 in the renewal or differentiation of stem cells and lineage-committed progenitors is clearly cell type and tissue dependent.

Integrative analysis of differential gene expression data from p53-null embryonic kidneys with p53 ChIP-Seq data has identified nearly 10% of the possible p53 target genes as enriched in the CM and nascent nephrons, indicating a substantial involvement of p53-mediated transcription in nephrogenesis (Li et al., 2013). To directly assess the contribution of p53 to NPC renewal and differentiation, we conditionally deleted p53 from the Six2^{+} CM. *Six2Cre*$^{+}$*;p53*$^{fl/fl}$ mice have hypoplastic kidneys and a nephron deficit (Saifudeen et al., 2012). Here, we show that the Six2(p53-null) CM exhibits a diminished NPC pool size and marked disorganization of the mesenchymal cells around the ureteric tip. The Cited1^{+} domain is completely lost by the time of birth. Further, adult mutant animals exhibit high blood pressure. RNA-Seq analysis of wild-type and mutant embryonic CM cells revealed that p53 is critically involved in regulation of cellular energy metabolism and cell adhesion pathways. These novel physiological functions of p53 on progenitor cell renewal, metabolism and adhesion have hitherto not been reported in a developing organ system.

RESULTS

A cell-autonomous requirement for p53 in self-renewal of the Cited1^{+}/Six2^{+} population

To determine the functional significance of p53 in the CM, we conditionally deleted p53 from the Six2^{+} mesenchyme by crossing *Six2-GFPCre* [*Six2*^{GC} (Kobayashi et al., 2008; Park et al., 2007)] to *p53*$^{loxP/loxP}$ mice to generate *Six2*$^{GC+}$*;p53*$^{loxP/loxP}$ mice (hereafter referred to as *Six2Cre*$^{+}$*;p53*$^{fl/fl}$). The breeding strategy used produced mutant and wild-type littermates of genotype *Six2*$^{GC+}$*;p53*$^{loxP/loxP}$ or *Six2*$^{GC-}$*;p53*$^{loxP/loxP}$ (*Six2Cre*$^{-}$*;p53*$^{fl/fl}$), respectively. Crosses of *Six2*$^{GC+}$*;p53*$^{+/+}$mice were performed to enable fluorescence activated cell sorting (FACS)-mediated isolation of p53-wild-type Six2(GFP^{+}) cells. Loss of p53 expression in the CM was confirmed by using real-time (RT)-PCR analysis (Fig. 1A) and subsequent RNA-Seq (below) (supplementary material Fig. S1).

The *Six2Cre*$^{+}$*;p53*$^{fl/fl}$ kidneys are hypoplastic as early as E13.5, with sparse, disorganized CM and UB-branching defects (Fig. 1B). This can also be visualized by using GFP fluorescence in *Six2Cre*$^{+}$*;p53*$^{+/+}$ and *Six2Cre*$^{+}$*;p53*$^{fl/fl}$ kidneys (Fig. 2A,B). Histological examination after Hematoxylin and Eosin staining draws attention to the absence of a clearly defined nephrogenic zone and a marked deficiency of differentiating nephrons in postnatal day 0 (P0) kidney sections (Fig. 1C), as well as an increase in interstitial stroma. Of

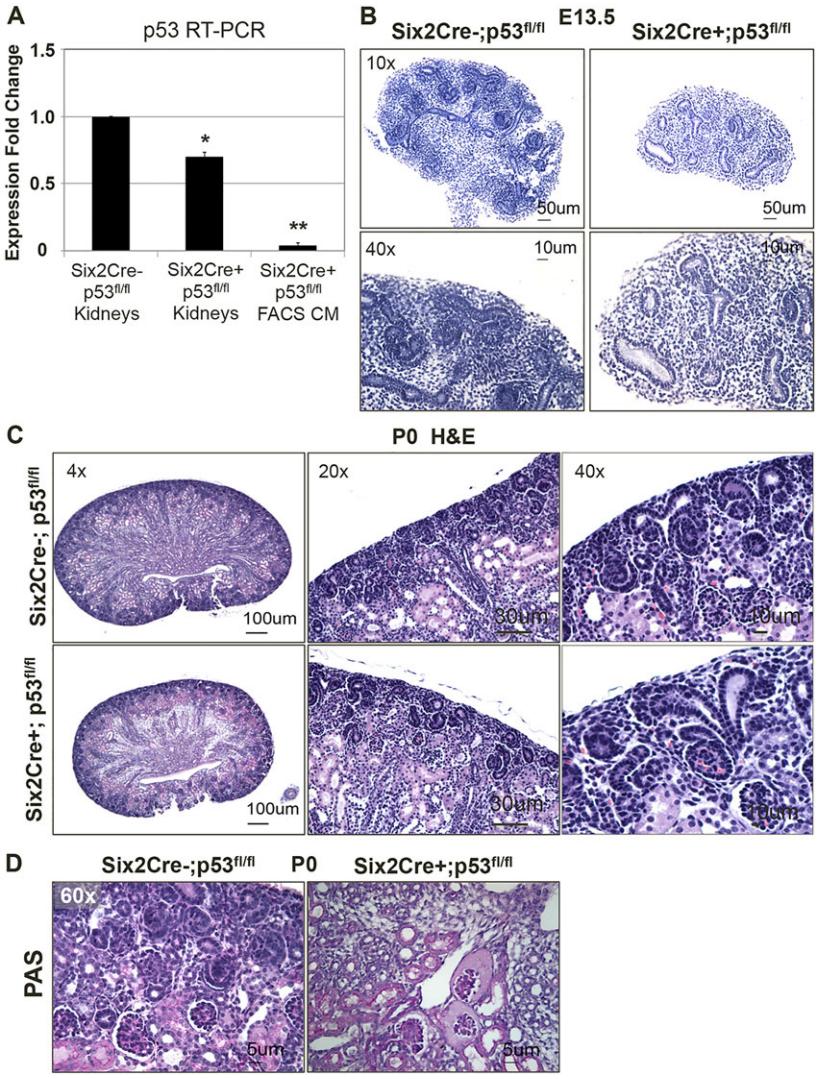

Fig. 1. Conditional deletion of p53 from the Six2^{+} mesenchyme. (A) RT-PCR was performed on RNA isolated from E15.5 *Six2Cre*$^{+}$*;p53*$^{fl/fl}$ kidneys or *Six2Cre*$^{+}$*;p53*$^{fl/fl}$ FACS-isolated cells to measure p53 expression. RNA from wild-type kidney was used as control. PCR primers spanned exon 9 to exon 10. (B) Hematoxylin and Eosin (H&E) staining of kidney sections at E13.5. Note hypoplasia, branching defects, dysmorphic CM and a paucity of nascent nephrons in mutant kidneys. (C) H&E staining of P0 kidney sections: note lack of a robust nephrogenic zone, nephron deficit and increased interstitial stroma (in 20× and 40× images). (D) PAS staining of P0 kidney sections: note the proteinaceous PAS-positive material in Bowman's space. Error bars represent s.e.m.; **P*<0.001, ***P*<0.001 (two-tailed *t*-test).

Development (2015) 142, 1228-1241 doi:10.1242/dev.111617

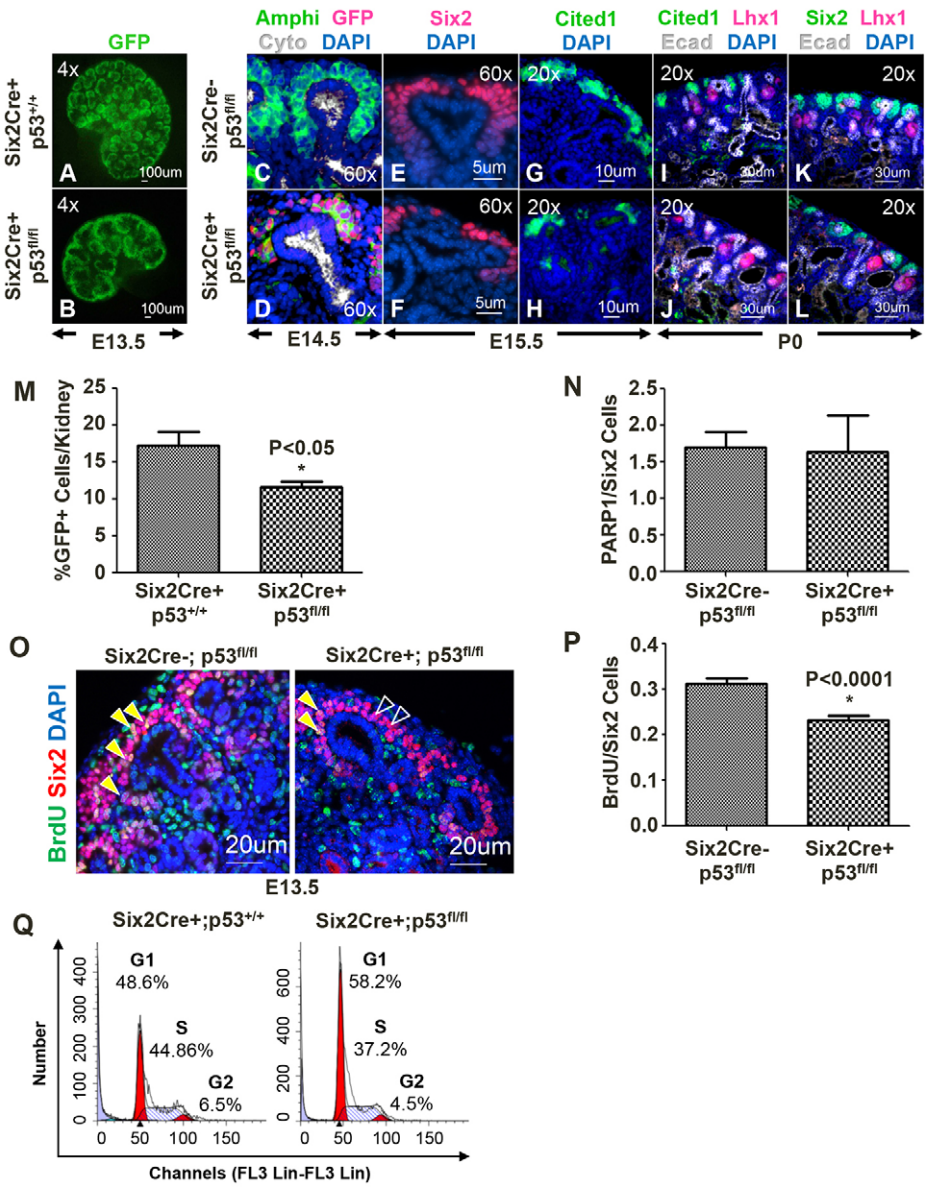

Fig. 2. Diminished CM and depletion of Cited1$^+$ progenitors in *Six2Cre$^+$;p53$^{fl/fl}$* kidneys. Wild-type and mutant littermate kidneys were examined. Genotypes are as shown. (A,B) GFP fluorescence highlights the Six2 cap. Hypoplasia is apparent at E13.5 in mutant kidneys. (C,D) Decreased expression of cap marker amphiphysin in mutant kidneys at E14.5. Note the disorganization of the mutant GFP-stained CM. Markers: UB (cytokeratin – cyto, white) and CM (amphiphysin – amphi, green); nuclear stain – DAPI, blue. (E-H) Diminished CM at E15.5 is demonstrated by Six2 (E,F) and Cited1 (G,H) immunofluorescence. Markers show epithelial structures (E-cadherin – Ecad, white) and nascent nephrons (Lhx1). (I-L) Cited1 marker is completely lost at P0 (I,J), whereas the Six2$^+$ domain is present but is greatly reduced (K,L). (M) Quantitation of Six2(GFP$^+$) cells from *Six2Cre$^+$;p53$^{+/+}$* and *Six2Cre$^+$;p53$^{fl/fl}$* kidneys at E15.5. Mutant kidneys have 30% fewer Six2(GFP$^+$) cells. FACS and quantitation was performed in three separate experiments, on embryos from three litters for each genotype. Bars in the graph show average cell count, with error bars denoting s.e.m. (N) Apoptosis, measured by immunostaining of PARP1 in kidney sections at E13.5-15.5, is lower in Six2$^+$ cells in *Six2Cre$^+$;p53$^{fl/fl}$* kidneys and does not contribute to the decrease in cap size in these kidneys. (O,P) Proliferative index measured by BrdU administration and immunostaining. BrdU incorporation was significantly lower in Six2$^+$ cells in *Six2Cre$^+$;p53$^{fl/fl}$* kidneys at E13.5 (P<0.001). BrdU was detected mostly in lateral section of the Six2$^+$ cap of the mutant kidney (solid yellow arrowheads), whereas the medial Six2$^+$ cells dorsal to the ureteric tip had few BrdU$^+$ cells (empty arrowheads). By contrast, wild-type kidney showed BrdU incorporation in all areas of the Six2$^+$ cap (yellow arrowheads). (Q) Cell cycle analysis of FACS-isolated GFP$^+$ cap cells demonstrates a decrease in the number of *Six2Cre$^+$;p53$^{fl/fl}$* cells in proliferative (S/G2/M) phases of the cell cycle compared with wild-type *Six2Cre$^+$;p53$^{+/+}$* cells. See Table 1 for quantitation (n=3, each genotype).

note are the glomeruli in PAS-stained P0 kidneys that display proteinaceous and/or hyaline material in Bowman's space, indicative of glomerular dysfunction (Fig. 1D). Immunofluorescent staining against the CM markers amphiphysin and Six2 accentuates the substantially diminished and less compact CM at E14.5-15.5 (Fig. 2C-F). Amphiphysin is a cell surface marker of the CM. The functional impact of a decrease of amphiphysin in a subset of *Six2Cre$^+$;p53$^{fl/fl}$* GFP$^+$ cells is not known at this time. GFP is expressed as a fusion protein with Cre and localizes to the nucleus and cytoplasm (Park et al., 2007). The diminished Cited1 domain is completely lost by P0 in *Six2Cre$^+$;p53$^{fl/fl}$* kidneys (Fig. 2G-J). Despite the loss of the Cited1$^+$ domain, Six2$^+$ cells persist at P0, when a markedly smaller Six2$^+$ CM is observed (Fig. 2K,L). In the absence of increased apoptosis (details below), an alternative

Development (2015) 142, 1228-1241 doi:10.1242/dev.111617

Table 1. Six2$^+$ CM cell cycle analysis

	Average±s.e. (%)		
Phase	p53 WT cap	p53 KO cap	*P*-value
G1/G0	50±2	58±3	0.014
G2/M	8±1	6±1	0.324
S	42±3	37±3	0.156
G2/S	50±2	42±3	0.014

KO, knockout; WT, wild type.

explanation for the presence of a smaller (but not absent) Cited1$^-$/Six2$^+$ population could be diminished self-renewal and premature exit of the Cited1$^+$ self-renewing cells to the transit, non-self-renewing pool (Cited1$^-$/Six2$^+$).

Flow cytometry analyses showed a significant (30%) decrease in Six2$^+$ cell number from mutant kidneys (n=3, P<0.05) (Fig. 2M). As stated above, this decrease is not due to increased apoptosis, as the apoptotic index (staining of PARP1) in the E13.5 CM was not different between *Six2Cre*$^+$;*p53*$^{fl/fl}$ and *Six2Cre*$^-$;*p53*$^{fl/fl}$ littermate kidneys (Fig. 2N). Paradoxically, p53 loss results in a significantly lower proliferative index of Six2 cells (Fig. 2O,P). Unlike in the wild-type CM, the S-phase marker BrdU was present predominantly in laterally located Six2$^+$ cells in *Six2Cre*$^+$;*p53*$^{fl/fl}$ kidneys, as opposed to the cells ventral to the ureteric tip (Fig. 2O). Cell cycle analysis showed that more *Six2Cre*$^+$;*p53*$^{fl/fl}$ cells were in the G1 phase, with a significantly smaller fraction in the S, G2 or M phases in comparison with the *Six2Cre*$^+$;*p53*$^{+/+}$ cells (Fig. 2Q, Table 1). Of note, the branching defect in the mutant kidneys affects niche number and, thereby, impacts the total Six2$^+$ cell number in these kidneys and, alongside the compromised proliferative capacity, is expected to contribute to the decreased count of mutant cells.

Six2Cre$^+$;*p53*$^{fl/fl}$ CM forms a less cohesive nephrogenic niche with loss of CM-stroma demarcation

In contrast to the compact aggregates of cap cells around the ureteric tip in wild-type kidneys, cells of the *Six2Cre*$^+$;*p53*$^{fl/fl}$ CM are dispersed and loosely organized around the ureteric tip (Fig. 3B,D). Immunostaining of neural cell adhesion molecule (NCAM1, referred to here as NCAM), which decorates the intercellular domains of CM and nascent nephrons, is greatly decreased in the mutant CM (Fig. 3C,D). NCAM is required for cell-cell and cell-matrix interactions during development and differentiation (Shin et al., 2002). The transcription factor Pax2 is expressed in both mesenchymal and UB lineages (Dressler et al., 1990); here, Pax2 expression was decreased in CM but not UB of *Six2Cre*$^+$;*p53*$^{fl/fl}$ kidneys (Fig. 3C,D), as described previously (Saifudeen et al., 2012). Another intriguing feature of the *Six2Cre*$^+$;*p53*$^{fl/fl}$ phenotype is the loss of demarcation between the CM and surrounding Meis1$^+$ cortical stroma, resulting in gaps between adjacent cap cells and between cap and UB cells, as well as the presence of stromal cells in close apposition to the UB tip (Fig. 3F, Fig. 2D), instead of a smooth uninterrupted CM adjacent to the UB (Fig. 3E).

Defects in progenitor cell renewal and mesenchyme to epithelial transition cause nephron deficit in *Six2Cre*$^+$;*p53*$^{fl/fl}$ kidneys

The *Six2Cre*$^+$;*p53*$^{fl/fl}$ kidneys exhibited a noticeable deficit in renal vesicles upon immunostaining for Lhx1$^+$ at E13.5 (Fig. 4A,B). Consequently, fewer LTA$^+$ proximal tubules and WT1$^+$ glomeruli were evident in P0 mutant kidneys (Fig. 4C,D). To determine whether nephron deficit in mutant kidneys was simply due to a decrease in NPC number or due to a possible defect in nephrogenesis, we induced canonical Wnt pathway-activated mesenchyme to epithelial transition (MET) in isolated Six2$^+$ NPCs. FACS-isolated Six2(GFP$^+$) cells from *Six2Cre*$^+$;*p53*$^{+/+}$ and *Six2Cre*$^+$;*p53*$^{fl/fl}$ kidneys were aggregated and cultured for a total of 48 h in medium supplemented with glycogen synthase kinase-3 inhibitor 6-bromoindirubin-3′-oxime (BIO) for the first 24 h followed by medium with vehicle (DMSO) for the subsequent 24 h, as described previously (Park et al., 2012). NPC that have been induced to differentiate through transient activation of the Wnt/β-catenin pathway express E-cadherin, indicative of MET. *Six2Cre*$^+$;*p53*$^{+/+}$ cells, upon induction, expressed E-cadherin and formed multicellular structures, as expected (Fig. 4G,I,K). By contrast, *Six2Cre*$^+$;*p53*$^{fl/fl}$ cells showed weak E-cadherin expression and failed to form complex structures (Fig. 4H,J,L), supporting the notion that defective MET is a contributor to the nephron deficit. Altogether, our data demonstrate that the nephron deficit in *Six2Cre*$^+$;*p53*$^{fl/fl}$ kidneys is due to at least two developmental defects: (a) impaired renewal of progenitor cells, and (b) a differentiation defect that is downstream of Wnt signaling which disrupts proper MET.

Therefore, next, we examined the expression of genes that are the earliest markers of nephrogenesis and are essential for MET. *In situ* hybridization analyses showed a clear decrease in *Fgf8*

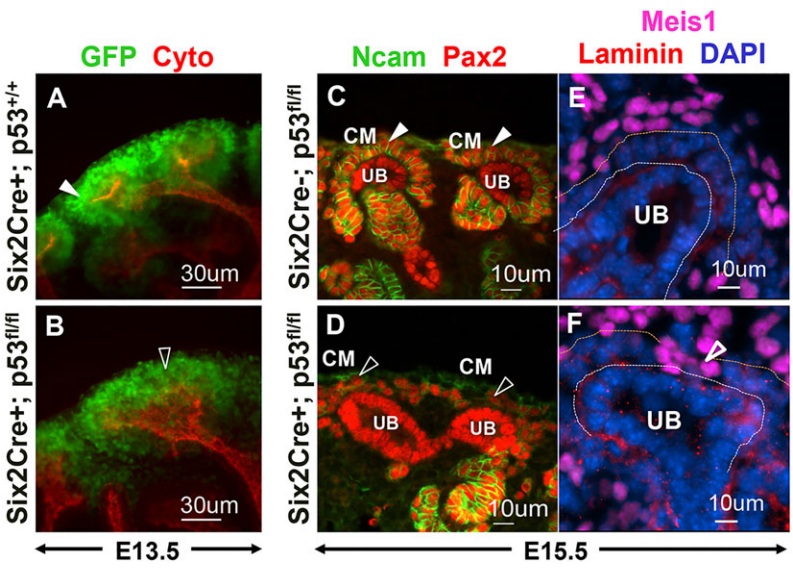

Fig. 3. Loss of CM integrity and disruption of the CM-stroma interface in *Six2Cre*$^+$;*p53*$^{fl/fl}$ kidneys. (A,B) *Six2Cre*$^+$;*p53*$^{fl/fl}$ cells are dispersed and loosely organized (empty arrowhead) around the ureteric tip, in contrast with *Six2Cre*$^+$;*p53*$^{+/+}$ cells, which are arranged compactly around the ureteric tip (solid white arrowhead). (C,D) Reduced NCAM expression in *Six2Cre*$^+$;*p53*$^{fl/fl}$ CM (empty arrowheads), in contrast to intense staining in wild-type CM (solid arrowheads). Pax2 expression is decreased in mutant CM. (E,F) Disruption of CM-UB and CM-stroma interfaces in *Six2Cre*$^+$;*p53*$^{fl/fl}$ kidneys. Immunostaining of Meis1 shows stromal cells infiltrating the *p53*$^{-/-}$ cap, and these cells are adjacent to the UB in mutant kidneys (empty arrowhead). Immunostaining of laminin demarcates the UB from the CM (white dotted line). The CM-stroma interface is shown with orange dotted line – this is disrupted in mutant kidneys.

Development (2015) 142, 1228-1241 doi:10.1242/dev.111617

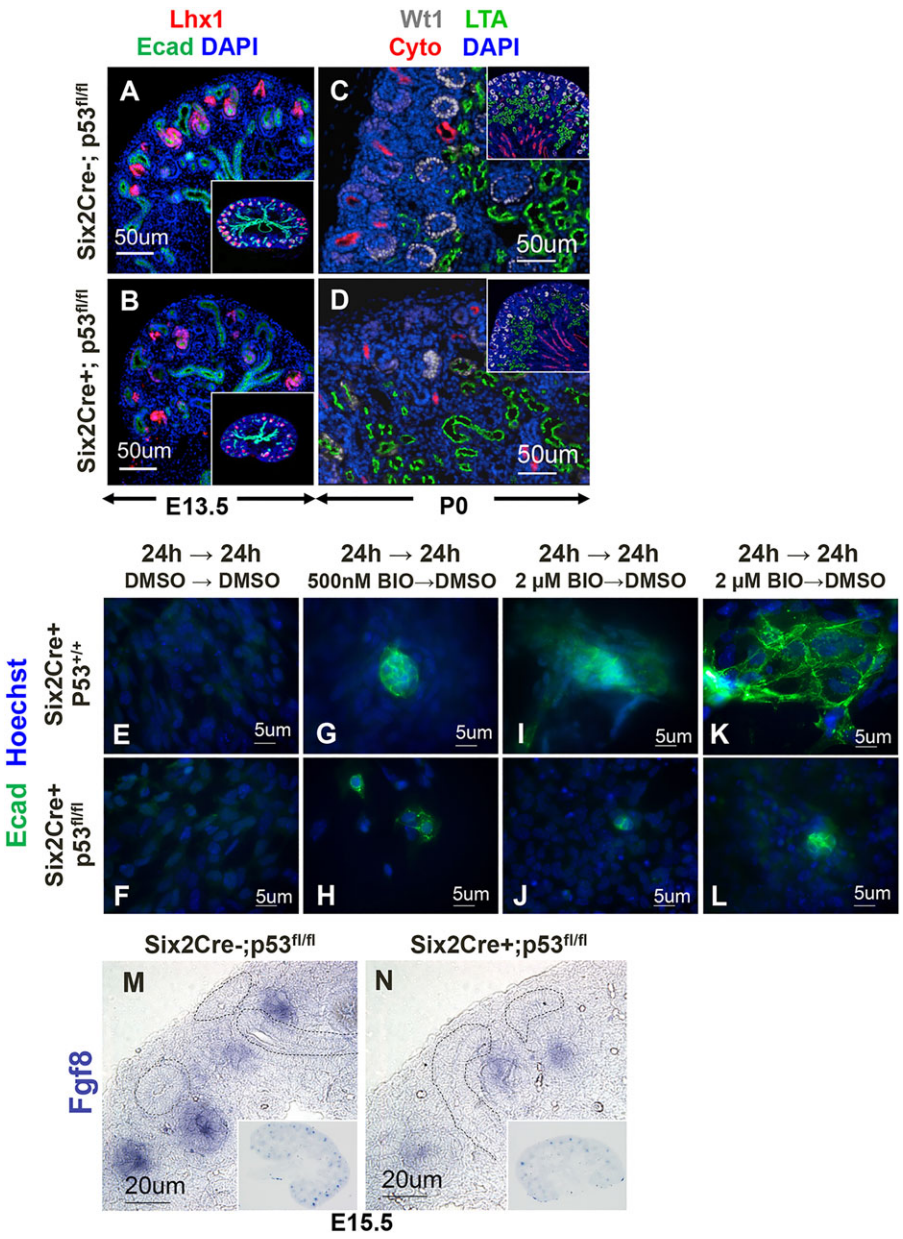

Fig. 4. Nephron deficit in *Six2Cre*$^{+}$;*p53*$^{fl/fl}$ kidneys. (A,B) Decrease in number and generations of Lhx1^{+} nascent nephrons in *Six2Cre*$^{+}$;*p53*$^{fl/fl}$ kidneys at E13.5 compared with littermate *Six2Cre*$^{-}$;*p53*$^{fl/fl}$ wild-type kidneys. UB branches and tips are shown by immunostaining of E-cadherin. Inset – low-power image. (C,D) Decrease in the number of mature nephrons in *Six2Cre*$^{+}$;*p53*$^{fl/fl}$ kidneys at P0 compared with littermate *Six2Cre*$^{-}$;*p53*$^{fl/fl}$ wild-type kidney. Inset – low-power image. Immunostaining for the following markers was performed: WT1 (low intensity staining in CM and nascent nephrons, and more intense staining of mature glomeruli in deeper cortex, white pseudocolor), LTA (proximal tubules, green) and cytokeratin (UB and collecting ducts, red). Hoechst (blue) was used to stain nuclei. (E-L) Impaired MET in *Six2Cre*$^{+}$;*p53*$^{fl/fl}$ kidneys. FACS-isolated CM cells from wild-type and mutant kidneys were pelleted and placed onto Transwell membranes and induced to differentiate with 500 nM or 2 μM BIO, as described in Materials and Methods. Wild-type cap cells upon induction express E-cadherin and form complex structures (G,I,K). *Six2Cre*$^{+}$;*p53*$^{fl/fl}$ cells showed some E-cadherin expression; however, they failed to form complex structures (H,J,L). DMSO (control)-treated cells never expressed E-cadherin. (M,N) Decreased Fgf8 expression in nascent nephrons of mutant kidneys at E15.5 (N), as visualized by using *in situ* hybridization. Inset shows low-power image.

mRNA in nascent nephrons in mutant kidneys (Fig. 4M,N). Decreased *Fgf8* expression was also observed by using RT-PCR analyses of RNA from mutant kidneys (data not shown). Surprisingly, however, expression of the tubulogenic factors Pax8 and Wnt4 did not show a marked change in expression (supplementary material Fig. S2). Expression of Fgf8 and Wnt4 has been shown to be concordant in the induced mesenchyme, and these factors function downstream of the inductive signal from Wnt9b (Carroll et al., 2005; Grieshammer et al., 2005; Perantoni et al., 2005). Wnt4 and Lhx1 are not expressed in Fgf8-null kidneys, and advanced epithelial structures do not form. Fgf8 hypomorphs express Wnt4 and Lhx1 and progress through nephrogenesis (Grieshammer et al., 2005). Despite being Fgf8 hypomorphs and expressing Wnt4 at normal levels, epithelialization occurs inefficiently in *Six2Cre*$^{+}$;*p53*$^{fl/fl}$ kidneys, indicating additional defects that impair differentiation of the *Six2Cre*$^{+}$;*p53*$^{fl/fl}$ CM. Indeed, addition of Fgf8-soaked beads to E13.5 *Six2Cre*$^{+}$;*p53*$^{fl/fl}$ kidneys did not facilitate even a partial rescue of nephrogenesis (supplementary material Fig. S3). Thus, whether defective MET in the mutant NPCs is a result of an impaired ability to be induced or of impaired epithelialization remains to be determined.

Elevated blood pressure in *Six2Cre*$^{+}$;*p53*$^{fl/fl}$ mice

Reduced nephron number from birth is strongly associated with the development of adult-onset diseases, such as hypertension (Brenner et al., 1988). Because both germline and conditional *p53*$^{-/-}$ mice exhibit impaired kidney development, renal hypoplasia and nephron deficit (Saifudeen et al., 2009, 2012; this study), we sought to determine the physiological impact of p53 loss on blood pressure. Continuous ambulatory blood pressure was monitored for 6 or 7 days in 2-month-old wild-type or mutant mice. The average time of tumor onset in *p53*$^{-/-}$ mice is ~3-4 months of age (Donehower, 1996). Younger mice could not be used because the small size of the mice increased the risk of death after implanting telemetry transmitters. Daytime blood pressure was significantly higher in *p53*$^{-/-}$ mice compared with that of wild-type mice (mean arterial pressure: 109.4±2.3 versus 95.5±1.1 mmHg, $P<0.05$, $n=6$ per

Development (2015) 142, 1228-1241 doi:10.1242/dev.111617

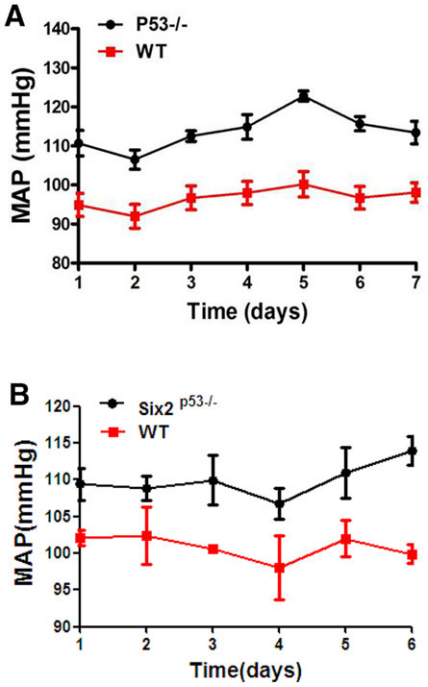

Fig. 5. Germline *p53*$^{-/-}$ and conditional *Six2Cre*$^{+}$*;p53*$^{fl/fl}$ mice have high blood pressure. (A) Daytime blood pressure is significantly higher in *p53*$^{-/-}$ mice compared to wild-type mice [mean arterial pressure (MAP): 109.4±2.3 versus 95.5±1.1 mmHg, $P<0.05$]. (B) *Six2Cre*$^{+}$*;p53*$^{fl/fl}$ mice have significantly higher blood pressure than wild-type mice (MAP: 110.0±0.97 versus 100.8±0.68 mmHg, $P<0.005$). Error bars indicate s.e.m.

genotype) (Fig. 5A), as it was in *Six2Cre*$^{+}$*;p53*$^{fl/fl}$ mice (mean arterial pressure: 110.0±0.97 versus 100.8±0.68 mmHg, $P<0.005$, $n=3$ per genotype) (Fig. 5B). These data implicate developmental defects in p53-deficient kidneys as an underlying cause of hypertension early in life.

Transcription profiles of *Six2Cre*$^{+}$*;p53*$^{+/+}$ and *Six2Cre*$^{+}$*;p53*$^{fl/fl}$ CM

To obtain a global transcription profile of *Six2Cre*$^{+}$*;p53*$^{+/+}$ and *Six2Cre*$^{+}$*;p53*$^{fl/fl}$ cells at E15.5, we utilized the Illumina TruSeq platform for paired-end RNA sequencing. Nearly 200 million total reads were obtained for each wild type and mutant (supplementary material Table S1). The expression of UB-specific genes (*Ret* and *Wnt9b*) was not detected, validating the enrichment of CM cells over UB lineage cells after FACS. Additionally, undetectable levels of reads from p53 exon 2 to exon 10 confirmed efficient deletion of this loxP-flanked fragment by Cre recombinase (supplementary material Fig. S1). RNA-Seq data was analyzed to obtain differential

Table 2. Expression of CM genes

Gene	Fold change (mut versus WT)	WT TPM	p53 mut TPM
Six2	1.1	451.2	501.5
Cited1	−1.3	104.6	78.2
Osr1	−1.3	65.8	52.6
Eya1	1.3	153.1	202.5
Gdnf	−1.04	51.5	49.4
Sall1	1.2	149.2	175.9
Meox1	−1.06	34.8	32.8
Wt1	−1.1	209.7	194.9
Crym	1.0	435.1	437.9

Mut, mutant; TPM, transcripts per million; WT, wild type.

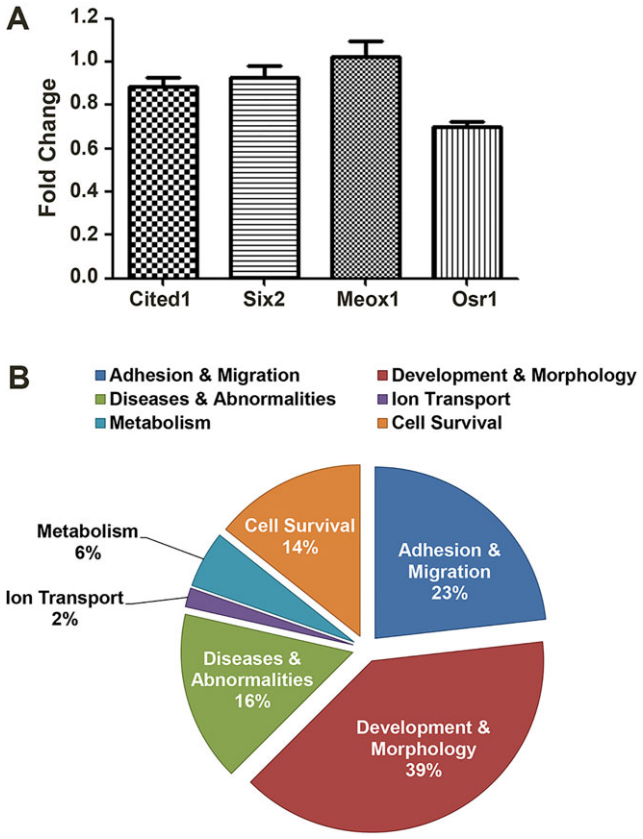

Fig. 6. *Six2Cre*$^{+}$*;p53*$^{fl/fl}$ CM gene expression. (A) RT-PCR analyses of mRNA from *Six2Cre*$^{+}$*;p53*$^{fl/fl}$ FACS-isolated CM cells confirms RNA-Seq expression data (Table 2) for *Six2* and *Meox1* expression (not decreased); *Cited1* and *Osr1* mRNA are decreased by 17% and 30%, respectively. Gene expression was normalized against mRNA levels for *Gapdh*. Error bars indicate s.e.m. (B) GO analysis of differentially expressed genes places them in six categories. IPA analysis predicted these categories to be substantially altered in *Six2Cre*$^{+}$*;p53*$^{fl/fl}$ cells.

expression using GeneSpring, and confirmed by using EBSeq and RSEM.

Six2 expression does not decrease in mutant CM (Table 2), confirmed by using RT-PCR (Fig. 6A), as well as immunostaining (Fig. 2F,L). A decrease in *Cited1* mRNA (−1.3 fold), as detected using RNA-Seq, in *Six2Cre*$^{+}$*;p53*$^{fl/fl}$ cells (Table 2) confirmed the decrease observed by using immunostaining (Fig. 2H). Decreased expression of other known CM genes (*GDNF*, *Sall1*, *Bmp7*, *Fgf20*, *Mdm2*, *Meox1*) (Table 2 and GEO accession GSE56253) was not detected, implicating a previously unidentified p53-mediated mechanism that is independent of these regulators in the maintenance of nephron progenitor cell number.

The top most downregulated genes included phosphoenol pyruvate carboxykinase 1 (*Pck1*, −14.3 fold), cytochrome P450 2D26 (*Cyp2d26*, −13.0 fold), meprin1a (*Mep1a*, −12.5 fold), aldolase b (*Aldob*, −12.0 fold), *Rec8* (−9.3 fold) and *Tmem174* (−9.0 fold). The most upregulated genes included *Fau* (4.3 fold), *Trim25* (2.2 fold) and *H2aZ* (*H2afz* – Mouse Genome Informatics; 1.9 fold). Fau is a fusion protein of an N-terminal ubiquitin-like protein Fubi fused to the ribosomal protein S30 at the C-terminal (Rossman et al., 2003). Trim25 belongs to the tripartite motif (TRIM) family and is an E3 ubiquitin ligase as well as a newly identified RNA-binding protein in mouse embryonic stem cells, suggesting a role in stem cell physiology (Kwon et al., 2013). H2AZ is a highly conserved histone variant that is essential for

Development (2015) 142, 1228-1241 doi:10.1242/dev.111617

Table 3. Ingenuity pathway analysis

Top categories		*P*-value
Diseases/ disorders	1. Metabolic	8.46×10^{-30}–2.87×10^{-8}
	2. Cardiovascular	7.07×10^{-29}–1.62×10^{-7}
	3. Cancer	3.82×10^{-26}–1.74×10^{-7}
Molecular and cellular functions	1. Cellular movement	3.28×10^{-38}–1.85×10^{-7}
	2. Growth and proliferation	7.54×10^{-32}–1.63×10^{-7}
	3. Cell morphology	1.88×10^{-31}–1.78×10^{-7}
	4. Cellular development	1.48×10^{-25}–1.63×10^{-7}
	5. Cell death and survival	1.06×10^{-24}–6.89×10^{-8}
Networks	1. Carbohydrate metabolism	
	2. Developmental, skeletal/muscle disorders	
	3. Connective tissue disorders	
	4. Cell movement and morphology	
	5. Lipid metabolism	

embryonic development in mice, and it might participate in telomere maintenance and regulate chromatin dynamics (Morillo-Huesca et al., 2010; Morrison and Shen, 2009).

Differentially expressed genes (supplementary material Table S2) were subjected to Gene Ontology (GO) analysis using the Ingenuity Pathway Analysis (IPA) software. Based on gene expression changes between wild-type and *Six2Cre*$^{+}$*;p53*$^{fl/fl}$ kidneys, IPA analysis predicted a significant alteration of function in six categories – development and morphology (39%), adhesion and migration (23%), diseases and abnormalities (16%), cell survival (14%), metabolism (6%) and ion transport (2%) (Fig. 6B). Enrichment analysis showed the highest enrichment of differentially expressed genes for (a) metabolic disorders; (b) cellular movement, growth and proliferation; and (c) carbohydrate and lipid metabolism (Table 3). A complete list of genes expressed in E15.5 Six2^{+} CM are posted on GEO under accession GSE56253.

The expression of several genes from the differential expression list were validated by using Nanostring nCounter digital gene expression analysis (Kulkarni, 2011). As shown by using nCounter quantification of mRNA expression in Fig. 7, a good correlation in expression trends between the RNA-Seq and nCounter data was obtained. The magnitude of fold change is higher with RNA-Seq, possibly from sensitivity and data normalization differences that exist between the two techniques.

Functional genomics implicate energy metabolism and cell adhesion as the drivers of the renal phenotype

Energy metabolism

The mRNA profile of *Six2Cre*$^{+}$*;p53*$^{fl/fl}$ cells revealed dysregulation of genes involved in glucose metabolism, the pentose phosphate pathway and the electron transport chain (ETC) (Table 4). The expression of several genes involved in ATP production, namely, components of the ETC or genes required to maintain a proton gradient for ATP production during oxidative respiration, was dysregulated. These are among the most downregulated genes in RNA-Seq data (Table 4). The decreased expression was confirmed by using quantitative nCounter

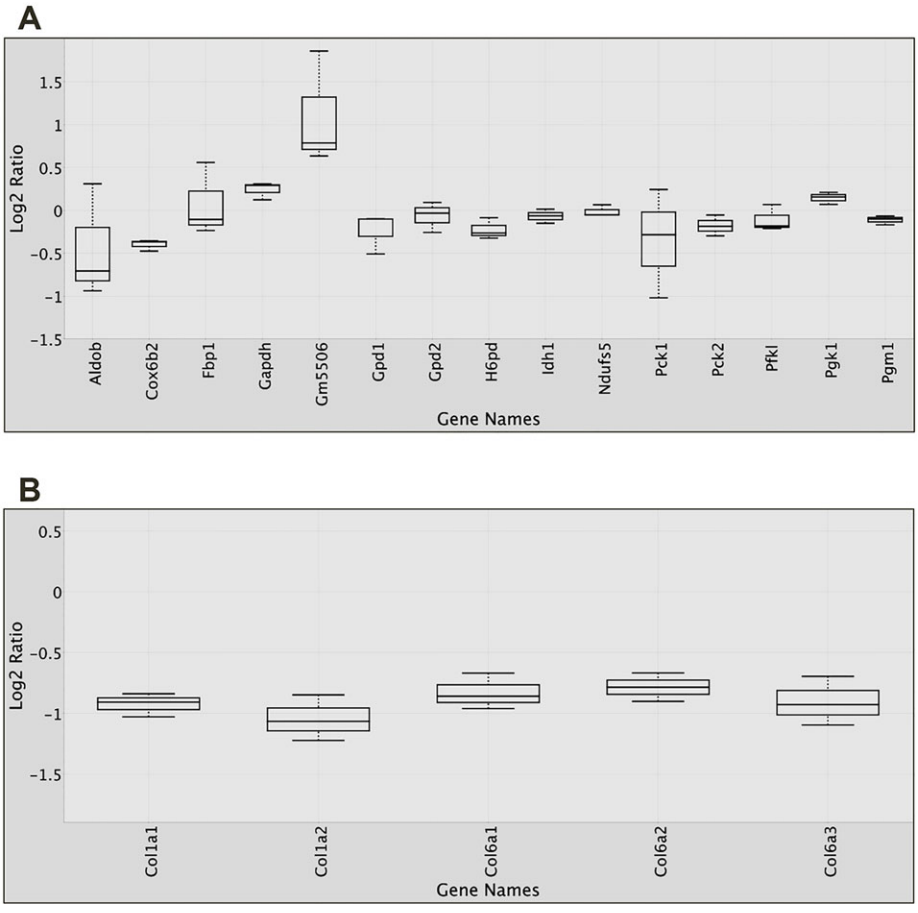

Fig. 7. Expression levels of genes involved in key energy metabolism and cell adhesion pathways. (A) Quantification of gene expression analysis by using Nanostring nCounter on mRNA from FACS-isolated *Six2Cre*$^{+}$*;p53*$^{fl/fl}$ CM cells. This analysis confirms the trend of RNA-Seq expression data for genes involved in energy metabolism pathways (Table 4). The magnitude of change in gene expression is different between the two techniques. Gm5506 codes for *Eno1b*. Gene symbols: *Aldob*, aldolase b; *Cox6b2*, cytochrome c oxidase subunit VIb polypeptide 2; *Fbp1*, fructose bisphosphatase 1; *Gapdh*, glyceraldehyde-3-phosphate dehydrogenase; *Gpd1*, glycerol-3-phosphate dehydrogenase 1 (soluble); *Gpd2*, glycerol phosphate dehydrogenase 2, mitochondrial; *H6pd*, hexose-6-phosphate dehydrogenase (glucose 1-dehydrogenase); *Idh1*, isocitrate dehydrogenase 1 (NADP^{+}), soluble; *Ndufs5*, NADH dehydrogenase (ubiquinone) Fe-S protein 5; *Pck1*, phosphoenolpyruvate carboxykinase 1, cytosolic; *Pck2*, phosphoenolpyruvate carboxykinase 2 (mitochondrial); *Pfkl*, phosphofructokinase, liver, B-type; *Pgk1*, phosphoglycerate kinase 1; *Pgm1*, phosphoglucomutase 1. (B) Confirmation of decreased expression of adhesion pathway genes in *Six2Cre*$^{+}$*;p53*$^{fl/fl}$ CM cells by using Nanostring nCounter gene expression analysis. Gene symbols: *Col1a1*, collagen, type I, α1; *Col1a2*, collagen, type I, α2; *Col6a1*, collagen, type VI, α1; *Col6a2*, collagen, type VI, α2; *Col6a3*, collagen, type VI, α3.

Development (2015) 142, 1228-1241 doi:10.1242/dev.111617

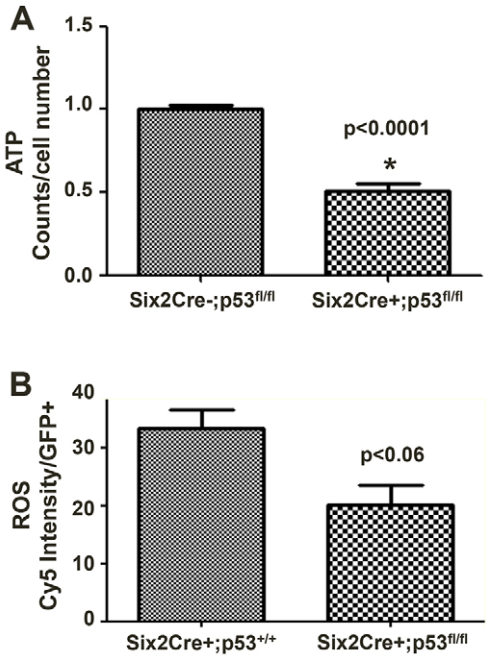

Fig. 8. Energy differences between wild-type and p53-null Six2^{+} cells. (A) ATP levels. mutant cells exhibit a significant, nearly 2-fold decrease in ATP levels than the wild-type cells (P<0.0001, n=3). ATP levels were assayed in duplicate from three independent pools, each of *Six2Cre*$^{-}$;*p53*$^{fl/fl}$ and *Six2Cre*$^{+}$;*p53*$^{fl/fl}$ cells. (B) ROS levels. ROS levels were consistently lower by ~30% in mutant cells. Cy5 intensity in GFP^{+} cells was measured in duplicate from three independent pools, each of *Six2Cre*$^{+}$;*p53*$^{+/+}$ and *Six2Cre*$^{+}$;*p53*$^{fl/fl}$ cells. Error bars indicate s.e.m.

expression analysis (Fig. 7), although the decrease was not of the same magnitude as that found by using RNA-Seq. Whether these genes are direct p53 targets in the CM remains to be determined. None of the tricarboxylic acid cycle (TCA) cycle enzymes showed expression changes.

Because of the indicated repression of energy pathways in *Six2Cre*$^{+}$;*p53*$^{fl/fl}$ cells from the gene expression data, we compared ATP levels between isolated E15.5 *Six2Cre*$^{-}$;*p53*$^{fl/fl}$ and *Six2Cre*$^{+}$;*p53*$^{fl/fl}$ cells. Mutant cells exhibited a significant, nearly 2-fold decrease in ATP levels than the wild-type cells (P<0.0001) (Fig. 8A). Because this could reflect mitochondrial dysfunction in *Six2Cre*$^{+}$;*p53*$^{fl/fl}$ cells, and because mitochondria are the major source of reactive oxygen species (ROS) (Holmström and Finkel, 2014), we measured ROS levels in these cells. ROS levels were consistently lower by ~30% in mutant cells (Fig. 8B). In summary, these data clearly indicate energy metabolism differences between wild-type and p53-deficient Six2^{+} cells and provide strong evidence of metabolic dysregulation of the p53-null CM.

Cell cycle and senescence pathways do not explain the *Six2Cre*$^{+}$;*p53*$^{fl/fl}$ renal phenotype

Expression of cell cycle inhibitors p21 (*Cdkn1a*) and p57 (*Cdkn1c*) was decreased and, thus, cannot account for the proliferation defect of the *Six2Cre*$^{+}$;*p53*$^{fl/fl}$ CM (supplementary material Table S3). Decreased proliferation might result from the unavailability of materials that are required for new cell synthesis, such as nucleotides, lipids and ATP. The downregulation of genes regulating amino acid metabolism, such as ornithine decarboxylase (*Odc1*, −1.6 fold) and arginine decarboxylase (*Adc*; *Azin2* – Mouse Genome Informatics; −1.6 fold), and contributing to polyamine synthesis was also observed. Polyamines are maintained within a very narrow range because a decrease in their concentrations inhibits cell proliferation, whereas excess appears to be toxic (Landau et al., 2012). Because decreased polyamine synthesis is usually observed in aging cells (Minois et al., 2011), we tested whether the *Six2Cre*$^{+}$;*p53*$^{fl/fl}$ cells were senescent. We found neither increased expression of cell cycle inhibitor p21 nor positive staining for senescence-associated β-galactosidase (SA-βgal) (supplementary material Fig. S4), indicating that the *Six2Cre*$^{+}$;*p53*$^{fl/fl}$ cells are not in replicative senescence.

DISCUSSION

The ability of p53 to restrict cell proliferation is associated with its well-characterized function as a tumor suppressor. Contrary to the prototypical roles of p53 in cancer and embryonic stem cells, our data point to a previously unknown role for p53 in enabling the renewal of multipotent progenitors in the nephrogenic niche. Mechanistically, our findings suggest that p53 is required to maintain energy metabolism and cell-matrix interactions, and consequently niche integrity. We propose that the absence of p53 triggers a 'metabolic crisis', resulting in loss of niche architecture, depletion of the self-renewing Cited1^{+} population and nephrogenesis defects that result in disease early in adulthood. Nephron progenitor loss in this conditional p53-deletion model is independent of apoptosis, cell senescence or impaired expression of known regulators of NPC maintenance and survival (Six2, Fgf20, Bmp7, Sall1, WT1 and Mdm2) (Barak et al., 2012; Basta et al., 2014; Blank et al., 2009; Hilliard et al., 2014; Kobayashi et al., 2008; Self et al., 2006).

In accord with the loosely organized CM in *Six2Cre*$^{+}$;*p53*$^{fl/fl}$ kidneys, RNA-Seq showed a high enrichment of altered gene expression in cell adhesion and migration pathways (Fig. 7B). These include genes encoding collagens, which contribute to the extracellular matrix, as well as genes involved in cytoskeletal remodeling (Table 5). Although the functions of many of the products of these genes in the NPC are unknown, disruption of biophysical and biomechanical cues from the extracellular matrix to cells within the niche can influence renewal and differentiation programs (Cox and Erler, 2011).

The *Six2Cre*$^{+}$;*p53*$^{fl/fl}$ kidneys clearly harbor fewer generations of nascent nephrons. However, unlike *Six2*, *Fgf9*, *Fgf20* or *Sall1* mutant kidneys (Barak et al., 2012; Basta et al., 2014; Self et al., 2006), the loss of Cited1^{+}/Six2^{+} progenitors in *Six2Cre*$^{+}$;*p53*$^{fl/fl}$ kidneys is not a result of precocious differentiation. No ectopic renal vesicles were visualized to suggest the smaller cap is due to advanced differentiation of progenitors. Indeed, this was not anticipated because Six2 expression is robust. The overall decrease in nephron number is multifactorial: impaired progenitor cell renewal, secondary UB branching defects and loss of the compact niche architecture, which disrupts the CM microenvironment and the signaling pathways between the CM and UB lineages and between the CM and stroma lineages (Fig. 9A) that are crucial for NPC renewal and differentiation (Das et al., 2013; Fetting et al., 2014). A simple decrease in proliferation would also result in fewer Six2^{+} cells, but not in the progressive loss and premature absence of Cited1^{+} cells observed here. The progressive loss of Cited1^{+} cells suggests a decreased capacity for self-renewal because, as per our current knowledge, Cited1 marks the self-renewing population. Proliferation of Six2^{+} cells (see BrdU staining, Fig. 2O) explains why Six2^{+} cells are not entirely lost by P0.

One of the most interesting findings of this study is that the top dysregulated genes belong to energy metabolism pathways. Enzyme deficiencies in metabolic pathways such as glycolysis, the TCA cycle and the ETC result in embryonic lethality (Kane and Buckley, 1977;

Development (2015) 142, 1228-1241 doi:10.1242/dev.111617

Table 4. Energy metabolism: gene expression in *Six2Cre^{+};p53$^{fl/fl}$* CM

Gene symbol	Fold change	Process	Function
Pck1	−14.3	Gluconeogenesis	Catalyzes the conversion of oxaloacetate (OAA) to phosphoenolpyruvate (PEP), the rate-limiting step in the metabolic pathway that produces glucose from lactate (Yu et al., 1993)
H6pd	−1.4	Pentose phosphate pathway (PPP)	Catalyzes the first two reactions of the PPP, thus generating NADPH (Hewitt et al., 2005); *H6pd* knockout mice have anomalies in glucose homeostasis and endoplasmic reticulum stress (Zielinska et al., 2011)
Gpd1	−2.1	Glycolysis, glycerol phosphate shunt, transfer of H^{+} to mitochondria	Forms the glycerol phosphate shuttle with mitochondrial GPD2, which facilitates the transfer of reducing equivalents (H^{+}) from the cytosol to mitochondria to maintain the proton gradient across the mitochondrial membrane (Ansell et al., 1997)
Pfkl	−1.2	Glycolysis	Key regulatory enzyme in glycolysis – catalyzes the irreversible conversion of fructose-6-phosphate to fructose-1,6-bisphosphate (Sola-Penna et al., 2010); encodes the liver isoform
Aldob	−12.1		Catalyzes the conversion of fructose-1,6-bisphosphate to glyceraldehyde 3-phosphate and dihydroxyacetone phosphate and participates in gluconeogenesis (Yañez et al., 2005)
Idh1	−1.4	Cytoplasmic NADPH production	Catalyzes the oxidative decarboxylation of isocitrate into α-ketoglutarate used in the TCA cycle, with $NADP^{+}$ as the electron acceptor (Kloosterhof et al., 2011)
Pdk1	−1.3	Pyruvate activation and consumption	Reversibly inactivates the mitochondrial pyruvate dehydrogenase (PDH) complex through phosphorylation; it might thereby alter the metabolite flux by altering the activity of PDH, which converts pyruvate to acetyl-CoA (Kaplon et al., 2013)
Dld	1.3		Component of the pyruvate dehydrogenase complex and the α-ketoglutarate dehydrogenase complex (Brown et al., 1994)
Ndufs5	−1.5	Complex I (ETC)	Belongs to first enzyme complex of the ETC
Ndufs6	−1.3		
Uqcr11	−1.2	Complex III (ETC)	Ubiquinol-cytochrome c reductase (Islam et al., 1997)
Cox5b	−1.5	Complex IV (ETC)	Belongs to the terminal enzyme complex IV of the ETC that transfers electrons from reduced cytochrome c to oxygen thus generating a proton electrochemical gradient across the inner mitochondrial membrane that is crucial for ATP generation (Li et al., 2006)
Cox6b2	−1.9		
Cox7c	−1.2		
Atp5e	−1.3	Complex V (ETC, ATP synthase)	Essential subunit in the biosynthesis and assembly of the F1 part of the mitochondrial ATP synthase complex V that catalyzes ATP synthesis from ADP, utilizing an electrochemical gradient of protons across the inner membrane during oxidative phosphorylation (Mayr et al., 2010)

Bold indicates expression verified by using Nanostring.

Rahman et al., 2014). These pathways support the production of intermediates that act as electron carriers, and they play an essential role in anabolic pathways, such as fatty acid and nucleotide biosynthesis, which are required components for cells undergoing proliferation. The balance of biomass synthesis versus energy production through glycolysis and oxidative respiration, respectively, is crucial for cell proliferation. Downregulation of TCA cycle genes blocks mitosis in *Caenorhabditis elegans* embryos (Rahman et al., 2014), whereas mitochondrial depolarization in HCT116 cells arrests cells in G1/S, as does reduction of ATP levels in *Drosophila* cells (Mandal et al., 2005; Mitra et al., 2009).

p53 counteracts aberrant proliferation via the inhibition of glycolysis and the stimulation of oxidative phosphorylation through direct regulation of TIGAR (also known as fructose-2,6-bisphosphatase) and Sco2, respectively (Bensaad et al., 2006; Matoba et al., 2006). p53 loss in cancer results in increased glucose metabolism by means of glycolysis over oxidative phosphorylation even under aerobic conditions, and is termed the Warburg effect (Vander Heiden et al., 2009). Unlike in cancer cells, nephron progenitors lacking p53 showed no alterations in expression of either TIGAR or Sco2. Rather, our data show transcriptional repression of mitochondrial respiration and glucose metabolism pathways. A recent study describes the ability of p53 to adaptively regulate mitochondrial respiration in *Drosophila* cells and to maintain the supercompetitive status of the Myc^{+} cells by enhancing the metabolic flux (de la Cova et al., 2014). Interestingly, p53 loss in these cells reduces their viability and results in impaired metabolism, as it does in *Six2Cre^{+};p53$^{fl/fl}$* cells, suggesting a cell context-dependent regulation of cellular processes. p53-mediated stress-induced competition has also been described in the mammalian hematopoietic system using a mosaic mouse model with graded levels of p53 activity (Bondar and Medzhitov, 2010). Here, competition did not involve apoptosis, rather, the outcompeted cell did not contribute to clonal expansion by dropping out of the proliferative pool. In this system, the outcompeted 'loser' cells undergo a permanent growth arrest and are refractory to growth factors. Interestingly, genes that control interactions of the cell with its environment, such as cell adhesion and migration, are implicated in competitive interactions. p53 knock down in hematopoietic stem cells (HSCs) demonstrates that p53 positively regulates self-renewal independently of apoptosis (Milyavsky et al., 2010). Self-renewal in the HSCs is dependent upon p53-mediated genome stability and the maintenance of DNA damage response. Although we did not observe an increase in foci of phosphorylated γH2Ax in *Six2Cre^{+};p53$^{fl/fl}$* CM (data not shown), an indicator of DNA damage, p53 might play a similar protective role in the nephron progenitors by providing metabolic stability to the NPCs under stress.

ATP is necessary to fuel cell proliferation, migration and adhesion. Energy depletion resulting from decreased ATP production provides a mechanistic link to the *Six2Cre^{+};p53fl/fl* CM phenotype, as does a decrease in ROS, an essential regulator of

Development (2015) 142, 1228-1241 doi:10.1242/dev.111617

Table 5. Adhesion and migration gene expression in *Six2Cre*$^{+}$;*p53*$^{fl/fl}$ CM

Gene	Fold change	WT TPM	KO TPM	Function
Ntn	–4.5	19.0	4.2	Netrin is thought to be involved in axon guidance, cell adhesion and cell migration during development (Sun et al., 2011)
Cdc42ep1	–2.5	5.5	2.2	Cdc42 effector proteins (Cdc42ep or CEPs) bind Cdc42 to induce cytoskeletal remodeling and cell shape changes (Hirsch et al., 2001)
Cdc42ep2	–2.0	2.2	1.1	
Cdc42ep5	–2.1	8.6	4.1	
Rock1	1.3	12.1	16.1	Protein serine/threonine kinases; key regulators of actin remodeling, cell polarity, focal adhesion formation, cell adhesion and motility (Shimizu et al., 2005)
Rock2	1.3	13.6	17.1	
Twist1	–2.6	3.6	1.4	Transcription factors that regulate genes involved in epithelial mesenchymal transition (EMT), mesenchymal cell lineage determination and differentiation (Ansieau et al., 2008)
Twist2	–2.7	3.5	1.3	
Dpp4	–4.1	6.6	1.6	Ubiquitous, membrane-bound enzyme that can modify growth regulators such as chemokines, cytokines and colony-stimulating factors in hematopoietic stem/progenitor cells (Ou et al., 2013)
Arhgap24	–1.9	10.5	5.6	A Rho GTPase-activating protein involved in actin remodeling, cell migration and cell polarity (Lavelin and Geiger, 2005)
Gng11	–1.9	9.8	5.1	A G-protein, γ subunit; participates in signal transduction and regulation of enzymes and ion channels (Ray et al., 1995)
Col1a1	–4.5	96.2	21.4	Component of the extracellular matrix (ECM) (Cox and Erler, 2011)
Col1a2	–3.5	104.5	29.7	
Col6a3	–4.3	10.4	2.4	
Col5a2	–2.1	13.3	6.3	
Col3a1	–3.9	169.0	43.4	

Bold indicates expression verified by using Nanostring. KO, knockout; TPM, transcripts per million; WT, wild type.

redox-dependent signaling that is crucial in neural and intestinal stem cell self-renewal, hematopoietic progenitor maturation in *Drosophila* and genomic stability (Holmström and Finkel, 2014). We propose that a niche-defined change in energy metabolism pathway usage would drive the Cited1^{+}/Six2^{+} self-renewing cells to Cited1^{-}/Six2^{+} transit cells (Fig. 9B, purple energy sign). Untimely alterations in energy metabolism pathways (Fig. 9B, yellow energy sign) could impair self-renewal and promote an en masse transition of Cited1^{+}/Six2^{+} cells to non-renewing Cited1^{-}/Six2^{+} cells, gradually resulting in the complete loss of Cited1^{+} cells but maintenance of Six2^{+} cells (expectedly fewer) (Fig. 9B). Indeed, the significant decrease in the expression of glycolysis pathway genes that has been reported in nephron progenitors at the end of nephrogenesis emphasizes the involvement of metabolic regulation in cell fate decisions (Brunskill et al., 2011), and whether p53 is involved in these temporal metabolic and cell fate decisions remains to be determined.

The energy metabolism model posits how the progenitor pool self-renews while simultaneously contributing to the differentiation-competent pool in the nephrogenic niche. p53 might play an adaptive role in the self-renewing Cited1^{+} progenitors, assimilating multiple external and internal cues into a homeostatic metabolic response in order to maintain a robust cell that is capable of self-renewing. Differences in cellular response might determine the continued participation of the Cited1^{+}/Six2^{+} cell in renewal or its exit to the transit Cited1^{-}/Six2^{+} population to undergo induction and differentiate. In this scenario, a p53-null cell would be refractory to external stimuli (positional, nutrient, mitogenic) and unable to modulate an internal metabolic response in order to fit the needs of the cells. Although this model points to a cell-intrinsic defect in the proliferation of *Six2Cre*$^{+}$;*p53*$^{fl/fl}$ cells, the defect might, in part, be cell extrinsic – for example, limited growth factor availability at the cell surface due to adhesion defects and inadequate or inappropriate cell-cell interactions (Fig. 9A). Premature entry of less fit cells into the non-renewing pool would result in a smaller pool of progenitors being available for nephrogenesis, leading to nephron deficit. However, this outcome protects the viability of the organism and could be more homeostatic than death of the unfit cells that would lead to either an extreme dearth or an absence of nephrons. Whether adhesion defects precede or follow the altered metabolism status of the mutant CM remains to be determined.

In summary, the present study demonstrates that p53 is required for the metabolic fitness of nephron progenitors and explains the apparent paradox of why p53 loss impeded rather than enhanced cell proliferation. p53 fulfills a physiological function in development and is required to maintain progenitor cell homeostasis. Further mechanistic studies to define the roles of p53, energy metabolism and cell adhesion and migration in self-renewal versus differentiation are ongoing.

MATERIALS AND METHODS

Transgenic mice

The *Six2*^{GC} transgenic mice express a GFP-fused Cre recombinase under the control of a Six2 BAC transgene [a gift from A. McMahon (Kobayashi et al., 2008; Park et al., 2007)]. *p53*$^{loxP/+}$ mice were obtained from Jackson Laboratories. *Six2*^{GC};*p53*$^{loxP/loxP}$ mice were crossed to *p53*$^{loxP/loxP}$ mice and embryonic kidneys harvested at desired time points. All animal protocols utilized in this study were approved by and in strict adherence to guidelines established by the Tulane University Institutional Animal Care and Use Committee.

CM cell isolation and culture from E15.5 kidneys

FACS

GFP^{+} kidneys were processed enzymatically to single cell suspensions for GFP-mediated FACS of p53-deleted Six2 cells (*Six2Cre*$^{+}$;*p53*$^{fl/fl}$). Wild-type GFP^{+} cells were similarly sorted from *Six2Cre*$^{+}$;*p53*$^{+/+}$ mice. Gating of GFP^{+} cells was performed based on control GFP^{-} cells. For quantification, CM cells were counted from pooled E15.5 kidneys from at least three litters of *Six2Cre*$^{+}$;*p53*$^{+/+}$ and *Six2Cre*$^{+}$;*p53*$^{fl/fl}$ embryos.

CM differentiation assay

Treatments using 500 nM and 2 µM BIO were performed as described previously (Park et al., 2012). Briefly, 1×10^{5} FACS-isolated *Six2Cre*$^{+}$;*p53*$^{fl/fl}$ or *Six2Cre*$^{+}$;*p53*$^{+/+}$ cells were pelleted and placed on a Transwell filter. DMEM/F12 medium with fetal bovine serum (FBS) was supplemented with BIO or DMSO. After 24 h, BIO medium was replaced with complete medium containing DMSO, for another 24 h. At this time, cells were fixed in 4% paraformaldehyde for 10 min and stained with an antibody against E-cadherin

Development (2015) 142, 1228-1241 doi:10.1242/dev.111617

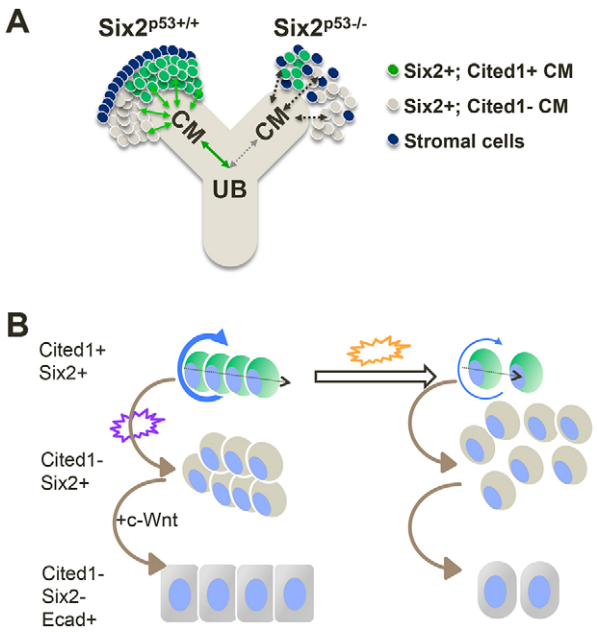

Fig. 9. Model for p53 function in NPC self-renewal and nephrogenesis. (A) Loss of self-renewing cells in *Six2Cre*$^{+}$*;p53*$^{fl/fl}$ CM. Cited1^{+} cells are lost (green circles) in *Six2Cre*$^{+}$*;p53*$^{fl/fl}$ CM. A Cited1^{-}/Six2^{+} domain (gray circles) is present, but with defects in organization and integrity loss. Stromal cells (navy blue circles) are interspersed in between the Six2^{+} cap cells. Thus, a distinct CM-stroma and CM-UB interface that is present in wild-type kidneys is lost in the Six2-p53-null kidneys. Disorganization of the niche would result in impaired signaling and cross-talk between the different lineages (denoted by dashed arrows in the *Six2Cre*$^{+}$*;p53*$^{fl/fl}$ CM). (B) A physiological change in energy metabolism pathway usage to drive the Cited1^{+}/Six2^{+} self-renewing cells (dotted arrow) to Cited1^{-}/Six2^{+} transit cells (purple energy flash sign) in normal development. An untimely change, however, in cellular metabolism of p53$^{-/-}$ Cited1^{+}/Six2^{+} cells (orange energy flash sign) might result in precocious arrest of self-renewal and an en masse transition to the Cited1^{-}/Six2^{+} non-renewing state. Adhesion defects could either precede or follow an altered metabolism status, resulting in a loose, disorganized CM that is unable to undergo efficient MET.

(1:200, 610181, BD Biosciences). Treatments using BIO were performed on three separate pools of FACS-isolated cells from three litters.

MACS

Manual magnetic-activated cell sorting (MACS) was used to sort Six2^{+} cells from E15.5 kidneys. Depletion of stromal, endothelial and erythroid cells was performed as previously described (Brown et al., 2013). Six2^{+} cells were isolated and plated in nephron progenitor expansion medium (NPEM) (A.B. and L.O., unpublished formulation) for the measurement of ATP levels.

Cell cycle analysis

Cell cycle analysis (n=3, each genotype) was performed on pools of 100,000 cells from embryos from multiple litters. FACS-isolated GFP^{+} *Six2Cre*$^{+}$*;p53*$^{fl/fl}$ or *Six2Cre*$^{+}$*;p53*$^{+/+}$ cells were fixed in ice-cold ethanol and stained with propidium iodide and treated with RNase A. The stained cells were loaded into the BD FACSArray bioanalyzer for DNA content-based cell cycle analysis.

Immunofluorescence immunohistochemistry

Kidneys at E15.5 were fixed in 10% formalin and processed for paraffin embedding and sectioning. Immunostaining was performed on 5 µm sections as previously described (Saifudeen et al., 2009). See supplementary material Methods for antibody information and image capture details. Whole-mount staining was performed on E12.5-13.5 kidneys, as previously described (Saifudeen et al., 2009). Staining for SA-βgal was performed on frozen tissue sections as per the manufacturer's protocol (BioVision). Hematoxylin and Eosin staining was performed on 5 µm paraffin-embedded tissue sections, as described previously (Cardiff et al., 2014). Periodic acid-Schiff (PAS) staining was performed as described previously (Saifudeen et al., 2009).

In situ hybridization

Section *in situ* hybridization was performed on paraffin-embedded kidney sections as described previously (Hilliard et al., 2014). The following cDNA probes were used: *Pax8* (from A. McMahon), *Wnt4* (from A. McMahon) and *Fgf8* (from Gail Martin and John Rubenstein).

Treatment with Fgf8 beads

PBS-washed Affigel Blue beads were soaked in recombinant Fgf8 (1 µg/ml, R&D Systems) for 30 min at 37°C, washed in PBS and placed on kidneys at E13.5 for 72 h. At this time, kidneys were fixed in 2% paraformaldehyde and stained with an antibody against Lhx1. Bovine serum albumin (BSA)-soaked beads were used as control.

Gene expression analysis

RNA-Seq

RNA was purified from Six2^{+} FACS-isolated cells from *Six2Cre*$^{+}$*;p53*$^{+/+}$ and *Six2Cre*$^{+}$*;p53*$^{fl/fl}$ kidneys at E15.5. Poly(A) RNA was selected for 100 bp/read paired-end Illumina TruSeq RNA-Seq on the HiSeq 2000 system. Sequence aligner Novoalign v2.08.02 was used to align the raw reads to mouse genome assembly GRCm38/mm10. The quality of raw reads was tested by using FastQC (Babraham Bioinformatics). Before analyzing differential gene expression between wild-type and mutant cells using the GeneSpring 12.5 NGS module, the following parameters were applied to the reads – 'Benjamini Hochberg FDR Multiple Testing' corrected P-value (Audic Cleverie Test) <0.05, and FPKM cutoff ≥3 on wild-type samples. FPKM reflects the normalized enrichment of a gene (Garber et al., 2011). TPM represents Transcript Per Million, which measures the abundance of gene transcripts (isoforms) according to RNA-Seq readout (Wagner et al., 2012). Fold change (knockout divided by wild type) cutoff was set to 1.5 for Ingenuity Pathway Analysis. Differential expression data was processed using GeneSpring, EBSeq or RSEM. Predicted genes and pseudo-genes were excluded to improve the accuracy of gene identification by IPA. Processed datasets are available in Gene Expression Omnibus (GEO accession number GSE56253). See supplementary material Methods for quality codes.

Nanostring nCounter expression analysis

Direct, digital detection of mRNA was performed using the nCounter Analysis System (Nanostring Technologies) as per the manufacturer's protocol (Geiss et al., 2008; Kulkarni, 2011). mRNA was pooled from wild-type or mutant kidneys from multiple litters, and at least three independent pools per genotype were processed for expression analysis. RNA was loaded at 100 ng per sample, hybridized with a custom gene expression codeset containing unique pairs of 35-50 bp reporter probes and biotin-labeled capture probes, in addition to positive and negative controls. Probe target sequences are listed in supplementary material Table S4. Three housekeeping genes were used for normalization: *B2m*, *Tbp* and *Pgk1*. Data analysis was performed using nSolver Analysis Software v2. All samples passed quality control; no sample was flagged. All samples were normalized to have the same geometric mean of counts of an nCounter-provided positive-control probe, which was spiked into all reactions. See supplementary material Methods for hybridization and processing details.

Quantitative RT-PCR

RT-PCR was performed on RNA from FACS-isolated *Six2Cre*$^{+}$*;p53*$^{+/+}$ and *Six2Cre*$^{+}$*;p53*$^{fl/fl}$ cells at E15.5 to determine the expression of the genes encoding p53, Cited1, Six2, Meox and Osr1. All primer probes for the TaqMan gene expression assay were purchased from Applied Biosystems. For p53 expression, primer-probes spanning exon 9 to exon 10 (Mm01337166-mH) were used. Reactions were prepared using the TaqMan RNA-to-CT 1-Step Kit and amplified using Stratagene Mx3000P and Mx3005P instruments.

Development (2015) 142, 1228-1241 doi:10.1242/dev.111617

Expression was normalized against endogenous *Gapdh* levels. Experimental and biological triplicates were applied.

Measurement of ATP levels

ATPlite (Perkin Elmer) luminescent assay was performed as per the manufacturer's instructions. This assay is based on light produced by conversion of Luciferin by Luciferase to Oxyluciferin in an ATP-dependent reaction. The emitted light is proportional to ATP concentration in the cell lysate. MACS-isolated *Six2Cre*$^{+}$*;p53*$^{fl/fl}$ or *Six2Cre*$^{-}$*;p53*$^{fl/fl}$ cells (2.5×10^{4}/well) were seeded onto an ATP-free microplate. At 18-20 h after seeding, cells were lysed in the well, and the luminescence was measured after the addition of substrate. Values were normalized to cell number. Multiple experiments were performed with cells isolated from different litters (n=3).

ROS measurement

5.0×10^{4} FACS-isolated *Six2Cre*$^{+}$*;p53*$^{fl/fl}$ or *Six2Cre*$^{+}$*;p53*$^{+/+}$ cells were seeded per Transwell membrane. At 24 h after plating, Cyto-ROX reagent (Invitrogen) with Cy5 label was added to the medium. After a 30 min uptake period, cells were washed twice in PBS, trypsinized and counted by using flow cytometry. GFP^{+} cells were counted and factored for Cy5 intensity.

Blood pressure measurements

Telemetry transmitters were implanted into the carotid arteries of 2-month-old *p53*$^{-/-}$ (n=6) and *p53*$^{+/+}$ (n=6) male mice on a C57BL/6 genetic background, as described previously (Li et al., 2012). After a 2-week recovery period post-surgery, blood pressure was recorded continuously for 7 days. *Six2Cre*$^{+}$*;p53*$^{fl/fl}$ and wild-type mice (n=3 per genotype) were monitored in a similar manner.

Acknowledgements

Our sincere appreciation to Dr Samir El-Dahr, for his insightful discussions and critical reading of the manuscript. We thank Dr Hua Lu for helpful discussions. We also thank Dr Erik Flemington at the Tulane Cancer Center and the COBRE Cancer Crusaders Next Generation Sequence Analysis Core for his assistance with bioinformatics [supported by the National Institute of General Medical Sciences of the National Institutes of Health under Award Number P20GM103518]. We thank Mylinh Bernardi at the Genomic and RNA Profiling Core at Baylor College of Medicine for her assistance with RNA-Seq and Nanostring nCounter gene expression analyses. Our thanks also to the Tulane Hypertension and Renal Centers of Excellence Molecular and Imaging Core and Mouse Phenotyping Core, and Dr Sylvia Hilliard for her assistance with the Fgf8 bead experiments.

Competing interests

The authors declare no competing or financial interests.

Author contributions

Z.S. designed the research; Y.L., J.L., W.L. and Z.S. performed the experiments; Y.L. and M.B. performed the bioinformatics; A.B., T.C., M.L., L.O. and Y.F. contributed reagents and crucial research tools; Y.L. and J.L. helped prepare figures; Y.L., J.L. and Y.F. helped with data analysis; Z.S. analyzed the data and wrote the paper.

Funding

This work was supported by the National Institutes of Health: Center of Biomedical Research Excellence funding to Z.S. [NIH-NIGMS P20RR017659]; PNCE Pilot Grant [NIH-NIDDK P50DK096373 to Z.S.]; and the National Institute of Diabetes and Digestive and Kidney Diseases (NIDDK) Diabetic Complications Consortium (DiaComp) [DK076169 to Z.S.]. Deposited in PMC for release after 12 months.

Supplementary material

Supplementary material available online at
http://dev.biologists.org/lookup/suppl/doi:10.1242/dev.111617/-/DC1

References

Amariglio, F., Tchang, F., Prioleau, M.-N., Soussi, T., Cibert, C. and Méchali, M. (1997). A functional analysis of p53 during early development of Xenopus laevis. *Oncogene* **15**, 2191-2199.

Ansell, R., Granath, K., Hohmann, S., Thevelein, J. M. and Adler, L. (1997). The two isoenzymes for yeast NAD+ -dependent glycerol 3-phosphate dehydrogenase encoded by GPD1 and GPD2 have distinct roles in osmoadaptation and redox regulation. *EMBO J.* **16**, 2179-2187.

Ansieau, S., Bastid, J., Doreau, A., Morel, A.-P., Bouchet, B. P., Thomas, C., Fauvet, F., Puisieux, I., Doglioni, C., Piccinin, S. et al. (2008). Induction of EMT by twist proteins as a collateral effect of tumor-promoting inactivation of premature senescence. *Cancer Cell* **14**, 79-89.

Armata, H. L., Golebiowski, D., Jung, D. Y., Ko, H. J., Kim, J. K. and Sluss, H. K. (2010). Requirement of the ATM/p53 tumor suppressor pathway for glucose homeostasis. *Mol. Cell. Biol.* **30**, 5787-5794.

Asker, C., Wiman, K. G. and Selivanova, G. (1999). p53-induced apoptosis as a safeguard against cancer. *Biochem. Biophys. Res. Commun.* **265**, 1-6.

Aylon, Y. and Oren, M. (2007). Living with p53, dying of p53. *Cell* **130**, 597-600.

Balaburski, G. M., Hontz, R. D. and Murphy, M. E. (2010). p53 and ARF: unexpected players in autophagy. *Trends Cell Biol.* **20**, 363-369.

Barak, H., Huh, S.-H., Chen, S., Jeanpierre, C., Martinovic, J., Parisot, M., Bole-Feysot, C., Nitschké, P., Salomon, R., Antignac, C. et al. (2012). FGF9 and FGF20 maintain the stemness of nephron progenitors in mice and man. *Dev. Cell* **22**, 1191-1207.

Basta, J. M., Robbins, L., Kiefer, S. M., Dorsett, D. and Rauchman, M. (2014). Sall1 balances self-renewal and differentiation of renal progenitor cells. *Development* **141**, 1047-1058.

Bensaad, K., Tsuruta, A., Selak, M. A., Vidal, M. N. C., Nakano, K., Bartrons, R., Gottlieb, E. and Vousden, K. H. (2006). TIGAR, a p53-inducible regulator of glycolysis and apoptosis. *Cell* **126**, 107-120.

Benz, K. and Amann, K. (2010). Maternal nutrition, low nephron number and arterial hypertension in later life. *Biochim. Biophys. Acta* **1802**, 1309-1317.

Blank, U., Brown, A., Adams, D. C., Karolak, M. J. and Oxburgh, L. (2009). BMP7 promotes proliferation of nephron progenitor cells via a JNK-dependent mechanism. *Development* **136**, 3557-3566.

Bondar, T. and Medzhitov, R. (2010). p53-mediated hematopoietic stem and progenitor cell competition. *Cell Stem Cell* **6**, 309-322.

Boyle, S., Misfeldt, A., Chandler, K. J., Deal, K. K., Southard-Smith, E. M., Mortlock, D. P., Baldwin, H. S. and de Caestecker, M. (2008). Fate mapping using Cited1-CreERT2 mice demonstrates that the cap mesenchyme contains self-renewing progenitor cells and gives rise exclusively to nephronic epithelia. *Dev. Biol.* **313**, 234-245.

Brenner, B. M., Garcia, D. L. and Anderson, S. (1988). Glomeruli and blood pressure: less of one, more the other? *Am. J. Hypertens.* **1**, 335-347.

Brown, G. K., Otero, L. J., LeGris, M. and Brown, R. M. (1994). Pyruvate dehydrogenase deficiency. *J. Med. Genet.* **31**, 875-879.

Brown, A. C., Adams, D., de Caestecker, M., Yang, X., Friesel, R. and Oxburgh, L. (2011). FGF/EGF signaling regulates the renewal of early nephron progenitors during embryonic development. *Development* **138**, 5099-5112.

Brown, A. C., Muthukrishnan, S. D., Guay, J. A., Adams, D. C., Schafer, D. A., Fetting, J. L. and Oxburgh, L. (2013). Role for compartmentalization in nephron progenitor differentiation. *Proc. Natl. Acad. Sci. USA* **110**, 4640-4645.

Brunskill, E. W., Lai, H. L., Jamison, D. C., Potter, S. S. and Patterson, L. T. (2011). Microarrays and RNA-Seq identify molecular mechanisms driving the end of nephron production. *BMC Dev. Biol.* **11**, 15.

Buchakjian, M. R. and Kornbluth, S. (2010). The engine driving the ship: metabolic steering of cell proliferation and death. *Nat. Rev. Mol. Cell Biol.* **11**, 715-727.

Cardiff, R. D., Miller, C. H. and Munn, R. J. (2014). Manual Hematoxylin and Eosin staining of mouse tissue sections. *Cold Spring Harb. Protoc.* **2014**, 655-658.

Carroll, T. J., Park, J.-S., Hayashi, S., Majumdar, A. and McMahon, A. P. (2005). Wnt9b plays a central role in the regulation of mesenchymal to epithelial transitions underlying organogenesis of the mammalian urogenital system. *Dev. Cell* **9**, 283-292.

Cicalese, A., Bonizzi, G., Pasi, C. E., Faretta, M., Ronzoni, S., Giulini, B., Brisken, C., Minucci, S., Di Fiore, P. P. and Pelicci, P. G. (2009). The tumor suppressor p53 regulates polarity of self-renewing divisions in mammary stem cells. *Cell* **138**, 1083-1095.

Cox, T. R. and Erler, J. T. (2011). Remodeling and homeostasis of the extracellular matrix: implications for fibrotic diseases and cancer. *Dis. Model. Mech.* **4**, 165-178.

Das, A., Tanigawa, S., Karner, C. M., Xin, M., Lum, L., Chen, C., Olson, E. N., Perantoni, A. O. and Carroll, T. J. (2013). Stromal-epithelial crosstalk regulates kidney progenitor cell differentiation. *Nat. Cell Biol.* **15**, 1035-1044.

de la Cova, C., Senoo-Matsuda, N., Ziosi, M., Wu, D. C., Bellosta, P., Quinzii, C. M. and Johnston, L. A. (2014). Supercompetitor status of drosophila myc cells requires p53 as a fitness sensor to reprogram metabolism and promote viability. *Cell Metab.* **19**, 470-483.

Donehower, L. A. (1996). The p53-deficient mouse: a model for basic and applied cancer studies. *Semin. Cancer Biol.* **7**, 269-278.

Dressler, G. R., Deutsch, U., Chowdhury, K., Nornes, H. O. and Gruss, P. (1990). Pax2, a new murine paired-box-containing gene and its expression in the developing excretory system. *Development* **109**, 787-795.

Fetting, J. L., Guay, J. A., Karolak, M. J., Iozzo, R. V., Adams, D. C., Maridas, D. E., Brown, A. C. and Oxburgh, L. (2014). FOXD1 promotes nephron progenitor differentiation by repressing decorin in the embryonic kidney. *Development* **141**, 17-27.

Gadea, G., de Toledo, M., Anguille, C. and Roux, P. (2007). Loss of p53 promotes RhoA ROCK-dependent cell migration and invasion in 3D matrices. *J. Cell Biol.* **178**, 23-30.
Garber, M., Grabherr, M. G., Guttman, M. and Trapnell, C. (2011). Computational methods for transcriptome annotation and quantification using RNA-seq. *Nat. Methods* **8**, 469-477.
Geiss, G. K., Bumgarner, R. E., Birditt, B., Dahl, T., Dowidar, N., Dunaway, D. L., Fell, H. P., Ferree, S., George, R. D., Grogan, T. et al. (2008). Direct multiplexed measurement of gene expression with color-coded probe pairs. *Nat. Biotechnol.* **26**, 317-325.
Grieshammer, U., Cebrián, C., Ilagan, R., Meyers, E., Herzlinger, D. and Martin, G. R. (2005). FGF8 is required for cell survival at distinct stages of nephrogenesis and for regulation of gene expression in nascent nephrons. *Development* **132**, 3847-3857.
Hartman, H. A., Lai, H. L. and Patterson, L. T. (2007). Cessation of renal morphogenesis in mice. *Dev. Biol.* **310**, 379-387.
Hewitt, K. N., Walker, E. A. and Stewart, P. M. (2005). Minireview: hexose-6-phosphate dehydrogenase and redox control of 11β-hydroxysteroid dehydrogenase type 1 activity. *Endocrinology* **146**, 2539-2543.
Hilliard, S. A., Yao, X. and El-Dahr, S. S. (2014). Mdm2 is required for maintenance of the nephrogenic niche. *Dev. Biol.* **387**, 1-14.
Hirsch, D. S., Pirone, D. M. and Burbelo, P. D. (2001). A new family of Cdc42 effector proteins, CEPs, function in fibroblast and epithelial cell shape changes. *J. Biol. Chem.* **276**, 875-883.
Holmström, K. M. and Finkel, T. (2014). Cellular mechanisms and physiological consequences of redox-dependent signalling. *Nat. Rev. Mol. Cell Biol.* **15**, 411-421.
Hoy, W. E., Hughson, M. D., Singh, G. R., Douglas-Denton, R. and Bertram, J. F. (2006). Reduced nephron number and glomerulomegaly in Australian Aborigines: a group at high risk for renal disease and hypertension. *Kidney Int.* **70**, 104-110.
Hoy, W. E., Bertram, J. F., Denton, R. D., Zimanyi, M., Samuel, T. and Hughson, M. D. (2008). Nephron number, glomerular volume, renal disease and hypertension. *Curr. Opin. Nephrol. Hypertens.* **17**, 258-265.
Islam, M. M., Suzuki, H., Yoneda, M. and Tanaka, M. (1997). Primary structure of the smallest (6.4-kDa) subunit of human and bovine ubiquinol-cytochrome c reductase deduced from cDNA sequences. *Biochem. Mol. Biol. Int.* **41**, 1109-1116.
Kane, M. T. and Buckley, N. J. (1977). The effects of inhibitors of energy metabolism on the growth of one-cell rabbit ova to blastocysts in vitro. *J. Reprod. Fertil.* **49**, 261-266.
Kaplon, J., Zheng, L., Meissl, K., Chaneton, B., Selivanov, V. A., Mackay, G., van der Burg, S. H., Verdegaal, E. M. E., Cascante, M., Shlomi, T. et al. (2013). A key role for mitochondrial gatekeeper pyruvate dehydrogenase in oncogene-induced senescence. *Nature* **498**, 109-112.
Karner, C. M., Das, A., Ma, Z., Self, M., Chen, C., Lum, L., Oliver, G. and Carroll, T. J. (2011). Canonical Wnt9b signaling balances progenitor cell expansion and differentiation during kidney development. *Development* **138**, 1247-1257.
Kloosterhof, N. K., Bralten, L. B. C., Dubbink, H. J., French, P. J. and van den Bent, M. J. (2011). Isocitrate dehydrogenase-1 mutations: a fundamentally new understanding of diffuse glioma? *Lancet. Oncol.* **12**, 83-91.
Kobayashi, A., Valerius, M. T., Mugford, J. W., Carroll, T. J., Self, M., Oliver, G. and McMahon, A. P. (2008). Six2 defines and regulates a multipotent self-renewing nephron progenitor population throughout mammalian kidney development. *Cell Stem Cell* **3**, 169-181.
Kulkarni, M. M. (2011). Digital multiplexed gene expression analysis using the nanoString nCounter system. *Curr. Protoc. Mol. Biol.* Chapter 25p, Unit 25B.10.
Kwon, S. C., Yi, H., Eichelbaum, K., Föhr, S., Fischer, B., You, K. T., Castello, A., Krijgsveld, J., Hentze, M. W. and Kim, V. N. (2013). The RNA-binding protein repertoire of embryonic stem cells. *Nat. Struct. Mol. Biol.* **20**, 1122-1130.
Landau, G., Ran, A., Bercovich, Z., Feldmesser, E., Horn-Saban, S., Korkotian, E., Jacob-Hirsh, J., Rechavi, G., Ron, D. and Kahana, C. (2012). Expression profiling and biochemical analysis suggest stress response as a potential mechanism inhibiting proliferation of polyamine-depleted cells. *J. Biol. Chem.* **287**, 35825-35837.
Lavelin, I. and Geiger, B. (2005). Characterization of a novel GTPase-activating protein associated with focal adhesions and the actin cytoskeleton. *J. Biol. Chem.* **280**, 7178-7185.
Lee, K.-H., Li, M., Michalowski, A. M., Zhang, X., Liao, H., Chen, L., Xu, Y., Wu, X. and Huang, J. (2010). A genomewide study identifies the Wnt signaling pathway as a major target of p53 in murine embryonic stem cells. *Proc. Natl. Acad. Sci. USA* **107**, 69-74.
Li, Y., Park, J.-S., Deng, J.-H. and Bai, Y. (2006). Cytochrome c oxidase subunit IV is essential for assembly and respiratory function of the enzyme complex. *J. Bioenerg. Biomembr.* **38**, 283-291.
Li, W., Peng, H., Cao, T., Sato, R., McDaniels, S. J., Kobori, H., Navar, L. G. and Feng, Y. (2012). Brain-targeted (pro)renin receptor knockdown attenuates angiotensin II-dependent hypertension. *Hypertension* **59**, 1188-1194.
Li, Y., Liu, J., McLaughlin, N., Bachvarov, D., Saifudeen, Z. and El-Dahr, S. S. (2013). Genome-wide analysis of the p53 gene regulatory network in the developing mouse kidney. *Physiol. Genomics* **45**, 948-964.
Liu, Y., Elf, S. E., Miyata, Y., Sashida, G., Liu, Y., Huang, G., Di Giandomenico, S., Lee, J. M., Deblasio, A., Menendez, S. et al. (2009). p53 regulates hematopoietic stem cell quiescence. *Cell Stem Cell* **4**, 37-48.
Luyckx, V. A. and Brenner, B. M. (2010). The clinical importance of nephron mass. *J. Am. Soc. Nephrol.* **21**, 898-910.
Mandal, S., Guptan, P., Owusu-Ansah, E. and Banerjee, U. (2005). Mitochondrial regulation of cell cycle progression during development as revealed by the tenured mutation in Drosophila. *Dev. Cell* **9**, 843-854.
Matoba, S., Kang, J.-G., Patino, W. D., Wragg, A., Boehm, M., Gavrilova, O., Hurley, P. J., Bunz, F. and Hwang, P. M. (2006). p53 regulates mitochondrial respiration. *Science* **312**, 1650-1653.
Mayr, J. A., Havlíčková, V., Zimmermann, F., Magler, I., Kaplanová, V., Ješina, P., Pecinová, A., Nůsková, H., Koch, J., Sperl, W. et al. (2010). Mitochondrial ATP synthase deficiency due to a mutation in the ATP5E gene for the F1 ε subunit. *Hum. Mol. Genet.* **19**, 3430-3439.
Meletis, K., Wirta, V., Hede, S.-M., Nistér, M., Lundeberg, J. and Frisén, J. (2006). p53 suppresses the self-renewal of adult neural stem cells. *Development* **133**, 363-369.
Milyavsky, M., Gan, O. I., Trottier, M., Komosa, M., Tabach, O., Notta, F., Lechman, E., Hermans, K. G., Eppert, K., Konovalova, Z. et al. (2010). A distinctive DNA damage response in human hematopoietic stem cells reveals an apoptosis-independent role for p53 in self-renewal. *Cell Stem Cell* **7**, 186-197.
Minois, N., Carmona-Gutierrez, D. and Madeo, F. (2011). Polyamines in aging and disease. *Aging (Albany NY)* **3**, 716-732.
Mitra, K., Wunder, C., Roysam, B., Lin, G. and Lippincott-Schwartz, J. (2009). A hyperfused mitochondrial state achieved at G1-S regulates cyclin E buildup and entry into S phase. *Proc. Natl. Acad. Sci. USA* **106**, 11960-11965.
Morillo-Huesca, M., Clemente-Ruiz, M., Andújar, E. and Prado, F. (2010). The SWR1 histone replacement complex causes genetic instability and genome-wide transcription misregulation in the absence of H2A.Z. *PLoS ONE* **5**, e12143.
Morrison, A. J. and Shen, X. (2009). Chromatin remodelling beyond transcription: the INO80 and SWR1 complexes. *Nat. Rev. Mol. Cell Biol.* **10**, 373-384.
Mugford, J. W., Yu, J., Kobayashi, A. and McMahon, A. P. (2009). High-resolution gene expression analysis of the developing mouse kidney defines novel cellular compartments within the nephron progenitor population. *Dev. Biol.* **333**, 312-323.
Olovnikov, I. A., Kravchenko, J. E. and Chumakov, P. M. (2009). Homeostatic functions of the p53 tumor suppressor: regulation of energy metabolism and antioxidant defense. *Semin. Cancer Biol.* **19**, 32-41.
Ou, X., O'Leary, H. A. and Broxmeyer, H. E. (2013). Implications of DPP4 modification of proteins that regulate stem/progenitor and more mature cell types. *Blood* **122**, 161-169.
Park, J.-S., Valerius, M. T. and McMahon, A. P. (2007). Wnt/β-catenin signaling regulates nephron induction during mouse kidney development. *Development* **134**, 2533-2539.
Park, J.-S., Ma, W., O'Brien, L. L., Chung, E., Guo, J.-J., Cheng, J.-G., Valerius, M. T., McMahon, J. A., Wong, W. H. and McMahon, A. P. (2012). Six2 and Wnt regulate self-renewal and commitment of nephron progenitors through shared gene regulatory networks. *Dev. Cell* **23**, 637-651.
Perantoni, A. O., Timofeeva, O., Naillat, F., Richman, C., Pajni-Underwood, S., Wilson, C., Vainio, S., Dove, L. F. and Lewandoski, M. (2005). Inactivation of FGF8 in early mesoderm reveals an essential role in kidney development. *Development* **132**, 3859-3871.
Rahman, M. M., Rosu, S., Joseph-Strauss, D. and Cohen-Fix, O. (2014). Down-regulation of tricarboxylic acid (TCA) cycle genes blocks progression through the first mitotic division in Caenorhabditis elegans embryos. *Proc. Natl. Acad. Sci. USA* **111**, 2602-2607.
Ray, K., Kunsch, C., Bonner, L. M. and Robishaw, J. D. (1995). Isolation of cDNA clones encoding eight different human G protein γ subunits, including three novel forms designated the γ4, γ10, and γ11 subunits. *J. Biol. Chem.* **270**, 21765-21771.
Rossman, T. G., Visalli, M. A. and Komissarova, E. V. (2003). fau and its ubiquitin-like domain (FUBI) transforms human osteogenic sarcoma (HOS) cells to anchorage-independence. *Oncogene* **22**, 1817-1821.
Rumballe, B. A., Georgas, K. M., Combes, A. N., Ju, A. L., Gilbert, T. and Little, M. H. (2011). Nephron formation adopts a novel spatial topology at cessation of nephrogenesis. *Dev. Biol.* **360**, 110-122.
Saifudeen, Z., Dipp, S., Stefkova, J., Yao, X., Lookabaugh, S. and El-Dahr, S. S. (2009). p53 regulates metanephric development. *J. Am. Soc. Nephrol.* **20**, 2328-2337.
Saifudeen, Z., Liu, J., Dipp, S., Yao, X., Li, Y., McLaughlin, N., Aboudehen, K. and El-Dahr, S. S. (2012). A p53-Pax2 pathway in kidney development: implications for nephrogenesis. *PLoS ONE* **7**, e44869.
Schoppy, D. W., Ruzankina, Y. and Brown, E. J. (2010). Removing all obstacles: a critical role for p53 in promoting tissue renewal. *Cell Cycle* **9**, 1313-1319.
Self, M., Lagutin, O. V., Bowling, B., Hendrix, J., Cai, Y., Dressler, G. R. and Oliver, G. (2006). Six2 is required for suppression of nephrogenesis and progenitor renewal in the developing kidney. *EMBO J.* **25**, 5214-5228.
Shimizu, Y., Thumkeo, D., Keel, J., Ishizaki, T., Oshima, H., Oshima, M., Noda, Y., Matsumura, F., Taketo, M. M. and Narumiya, S. (2005). ROCK-I regulates

closure of the eyelids and ventral body wall by inducing assembly of actomyosin bundles. *J. Cell Biol.* **168**, 941-953.

Shin, M. H., Lee, E.-G., Lee, S.-H., Lee, Y. S. and Son, H. (2002). Neural cell adhesion molecule (NCAM) promotes the differentiation of hippocampal precursor cells to a neuronal lineage, especially to a glutamatergic neural cell type. *Exp. Mol. Med.* **34**, 401-410.

Sola-Penna, M., Da Silva, D., Coelho, W. S., Marinho-Carvalho, M. M. and Zancan, P. (2010). Regulation of mammalian muscle type 6-phosphofructo-1-kinase and its implication for the control of the metabolism. *IUBMB Life* **62**, 791-796.

Sun, K. L. W., Correia, J. P. and Kennedy, T. E. (2011). Netrins: versatile extracellular cues with diverse functions. *Development* **138**, 2153-2169.

Tasdemir, E., Maiuri, M. C., Galluzzi, L., Vitale, I., Djavaheri-Mergny, M., D'Amelio, M., Criollo, A., Morselli, E., Zhu, C., Harper, F. et al. (2008). Regulation of autophagy by cytoplasmic p53. *Nat. Cell Biol.* **10**, 676-687.

Vander Heiden, M. G., Cantley, L. C. and Thompson, C. B. (2009). Understanding the warburg effect: the metabolic requirements of cell proliferation. *Science* **324**, 1029-1033.

Vousden, K. H. and Prives, C. (2009). Blinded by the light: the growing complexity of p53. *Cell* **137**, 413-431.

Wagner, G. P., Kin, K. and Lynch, V. J. (2012). Measurement of mRNA abundance using RNA-seq data: RPKM measure is inconsistent among samples. *Theory Biosci.* **131**, 281-285.

Wlodek, M. E., Westcott, K., Siebel, A. L., Owens, J. A. and Moritz, K. M. (2008). Growth restriction before or after birth reduces nephron number and increases blood pressure in male rats. *Kidney Int.* **74**, 187-195.

Xu, Y. (2005). A new role of p53 in maintaining genetic stability in embryonic stem cells. *Cell Cycle* **4**, 363-364.

Yañez, A. J., Ludwig, H. C., Bertinat, R., Spichiger, C., Gatica, R., Berlien, G., Leon, O., Brito, M., Concha, I. I. and Slebe, J. C. (2005). Different involvement for aldolase isoenzymes in kidney glucose metabolism: aldolase B but not aldolase A colocalizes and forms a complex with FBPase. *J. Cell. Physiol.* **202**, 743-753.

Yu, H., Thun, R., Chandrasekharappa, S., Trent, J. M., Zhang, J. and Meisler, M. H. (1993). Human PCK1 encoding phosphoenolpyruvate carboxykinase is located on chromosome 20q13.2. *Genomics* **15**, 219-221.

Zielinska, A. E., Walker, E. A., Stewart, P. M. and Lavery, G. G. (2011). Biochemistry and physiology of hexose-6-phosphate knockout mice. *Mol. Cell. Endocrinol.* **336**, 213-218.